

NOT SELECTED FOR  
CIRC/FWW

# AIR TECHNICAL INTELLIGENCE TRANSLATION

AD 676241

(Title Unclassified)  
INTERIOR BALLISTICS

by

M. E. Serevryakov

State Printing House of the  
Defense Industry

Moscow, 1949, 2nd Edition

672 Pages

(Part 3 of 10 Parts,  
Pages 173-269)



## MASTER

OCT 22 1968

### AIR TECHNICAL INTELLIGENCE CENTER

WRIGHT-PATTERSON AIR FORCE BASE

OHIO

NAD-83064  
F-TS-7327/V

This document has been approved  
for public release and sale; its  
distribution is unlimited

Reproduced by the  
CLEARINGHOUSE  
for Federal Scientific & Technical  
Information Springfield Va 22151

INTERIOR BALLISTICS

BY

M. E. SEREVRYAKOV

STATE PRINTING HOUSE OF THE DEFENSE INDUSTRY

MOSCOU, 1949, 2ND EDITION

672 PAGES

(PART 3 OF 10 PARTS, PP 175-269)

P-TS-7327/V  
NAD-83064

# SECTION III - BALLISTIC ANALYSIS OF POWDERS ON THE BASIS OF THE PHYSICAL LAW OF COMBUSTION

## CHAPTER I - METHOD FOR THE BALLISTIC ANALYSIS OF POWDERS

### 1. AN ATTEMPT TO CORRELATE THE THEORETICAL LAW WITH BOMB TESTS.

Formula  $dp/dt = T_p$  derived in the preceding chapter for tubular powders shows that  $dp/dt$  increases in proportion with  $p$ , and inasmuch as  $p$  itself continues to increase until the end of burning, the slope angle of the  $dp/dt$  curve must theoretically continue to increase also.

Nevertheless, in all the  $p, t$  curves obtained in burning powders in a manometric bomb, the maximum slope angle is obtained not at the maximum pressure at the end of the curve but, rather, at some  $p_i < p_m$ . The point of inflexion  $i$  corresponds to pressure  $p_i$ , following which the  $p, t$  curve becomes concave instead of convex, and often approaches the end of burning when  $dp/dt \approx 0$  (for strip and tubular powders).

The validity of the geometric law of burning was questioned for the first time by Charbonier, who attempted to investigate real powders and all their defects peculiar to manufacturing processes.

Using for his observations an imperfect cylindrical crusher and analyzing the shape of the pressure curves obtained in a manometric bomb, Charbonier introduced a special "shape function" to account for the actual burning of the powder, which was supposed to represent an analytical expression linking the relative surface area  $S/S_1$  with the burned portion of the charge  $\psi$ .

The exponent of this function was determined not by the shape of the grain but, rather, on the basis of the bomb test.

NAO 83064

#### A. Derivation of a General Formula for the Shape Function

Let us find the relation between the value of the surface area ratio  $S/S_1$  at a given instant and the burned portion of the charge  $\psi$  for powders of the simplest shapes: for a sphere burning in parallel layers towards the center, for a solid cylinder, and for an infinitely wide strip.

a) Sphere. The initial volume of the sphere is  $\Lambda_1 = 4/3\pi R^3$  (fig. 43). The volume of the burned portion  $\Lambda_{cr} = \Lambda_1 - \Lambda_{ocr} = \frac{4}{3}\pi(R^3 - r^3)$ . The burned portion of the grain

$$\psi = \Lambda/\Lambda_1 = 1 - \frac{\Lambda_{ocr}}{\Lambda_1} = 1 - \left(\frac{r}{R}\right)^3. \quad (45)(*)$$

The initial surface area  $S_1 = 4\pi R^2$ . The area at the given instant is  $S = 4\pi r^2$ .

Therefore,

$$\frac{S}{S_1} = \left(\frac{r}{R}\right)^2. \quad (46)$$

Eliminating  $\frac{r}{R}$  from (45) and (46), we get:

$$\frac{S}{S_1} = (1 - \psi)^{\frac{2}{3}}. \quad (47)$$

---

(\*) Subscript  $cr$  = abbreviation of the word burned, subscript  $ocr$  = abbreviation of the word remainder - translator.

# GRAPHIC NOT REPRODUCIBLE

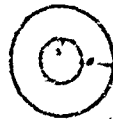


Fig: 43 - Burning Diagram for a Sphere (a Right Circular Cylinder).

b) Solid cylinder. Let the height of the cylinder  $h$  be great in comparison with its diameter and let us assume that the effect produced by the decrease in length on the volume change may be disregarded.

Then, referring to fig. 43:

$$\Lambda_1 = \pi R^2 h; \quad \Lambda_{cr} = \pi(R^2 - r^2) h;$$

$$S = 2\pi r h; \quad S_1 = 2\pi R h;$$

$$\psi = 1 - \left(\frac{r}{R}\right)^2; \quad \frac{S}{S_1} = \frac{r}{R}.$$

Cancelling  $r/R$  from the expression for  $\psi$  and  $S/S_1$ , we get

$$\frac{S}{S_1} = (1 - \psi)^{1/2}.$$

c) Infinitely wide strip (the effect produced by the changes along the edges may be disregarded). The surface  $S$  remains constant, i.e.,  $S/S_1 = 1$ , and we can write:

$$S/S_1 = (1 - \psi)^0 = 1.$$

Thus in the case of typical regressive powder shapes the value of the area ratio  $S/S_1$  is expressed as a function of the same kind

$$S/S_1 = (1-\psi)^\beta,$$

where the exponent  $\beta = 2/3$  for a sphere,  $\beta = 1/2$  for a cylinder,  $\beta = 0$  for an infinite strip (powder with a constant burning area).

Actually of course the burning of powder deviates from this ideal law, and Charbonier had determined the  $\beta$  exponent from an actual bomb test, by setting on the  $p, t$  curve the maximum pressure  $p_m$  and pressure  $p_i$  at the point of inflexion:

$$\beta = \frac{p_m - p_i}{p_i} \quad (48)$$

The more uniform will be the burning of the powder, the higher will be the point of inflexion, the smaller the numerator, and the closer will the denominator and  $\beta$  exponent approach zero, and the more will the burning approach the condition of burning with a constant surface:

$$p_i = \frac{p_m}{1 + \beta}.$$

For a sphere  $p_i = 3/5 p_m$ ;

For a slab  $p_i = 2/3 p_m$ ; for  $\beta = 0$   $p_i = p_m$ .

For French cannon strip-type powders "B" it was determined by actual tests that  $\beta = 0.2$  and for rifle plate-type powder BF -  $\beta = 0.5$ . This shows that in actual practice plate powders burn similarly to a

theoretical solid cylinder of the more regressive type. The curve  $\sigma = (1-\psi)\beta$  when  $\beta = 0.2$  and  $0.5$  is shown in fig. 45 (curves 1 and 2).

The  $\sigma$ ,  $\psi$  curves for the same powder shapes burned according to the geometric law are shown in fig. 45 in the form of a dotted line (1' - strip, 2' - plate). Curves 1 and 2 are arranged below curves 1' and 2', respectively.



Fig. 44 - p, t Curve With a Point of Inflexion.

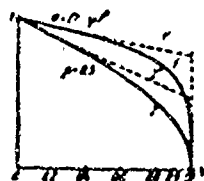


Fig. 45 - Shape Function  $\sigma = f(\psi)$ .

According to Charbonier: 1) surface  $y$  in all powders tends toward zero at the end of burning (because when  $\psi = 1$ ,  $\sigma = 0$ ), whereby this sharp surface reduction starts the sooner, the more regressive is the powder; 2) the actual burning of the powder is more regressive than it should be according to the geometric law; 3) the possible reason thereof is the heterogeneity of the mass and the nonsimultaneous ignition of all the elements of the charge.

At the same time his investigations made it possible to establish a connection between the theoretical formula and the experimental data, using for this purpose the p, t curve for pressure increase, obtained by burning powder in a manometric bomb.

Thus Charbonier had introduced an evaluation of the progressivity of burning on the basis of bomb tests rather than on the basis of the powder shape, and had concluded correctly that the progressivity of the shape does not fully determine the progressivity of burning - a process depending not only on the geometry of the grain, but also on the physical and chemical properties and conditions of loading and ignition.

At the same time the "snape function" which is a step forward as regards the evaluation of the nature of burning, still does not sufficiently reflect the latter, inasmuch as of the entire pressure test curve  $p, t$  only two points were utilized for the determination of  $\beta$ : point  $p_m$  at the end of burning and point  $p_i$  which is also close to the end of burning. The basic part of the curve was not utilized; this is partly explained by the fact that the curve was recorded by means of cylindrical crushers, and hence its form at the start of burning was unknown.

Nevertheless, maximum pressure is usually obtained in a gun after about half of the charge is burned, and hence the nature of burning from the start to the instant when the first half of the charge is burned must influence both the position of the maximum pressure in a gun as well as its magnitude. Actually, of course, the position of the inflexion point on the pressure curve in a bomb may not be closely associated with the first half of the burning process.

Therefore, the defect of the Charbonier method lies in the fact that the pressure curve remains unused on the whole.



In 1923-1924 M.E. Serebriakov obtained by means of a conical crusher full curves of the pressure increase of powder gases obtained by burning powder in a manometric bomb, and developed a new method for the analysis of powder burning utilizing the entire pressure curve for the purpose.

This analysis is conducted on the basis of the test characteristic of the burning progressivity of powder,  $\sqrt[4]{P}$ . This characteristic is obtained by sectional analysis of the entire pressure curve from the start to the end of burning; it shows the change in the intensity of gas formation during the entire burning process.

Using this method, a series of new hitherto unknown peculiarities were disclosed of the actual process of powder burning and its deviation from the geometric law; also proven by means of direct tests were some of the formulations originally assumed by Charbonier.

The principles of this method follow.

## 2. TEST CHARACTERISTIC " $\Gamma$ " OF THE PROGRESSIVE BURNING OF POWDER

### The Use of Function $\Gamma$ for the Analysis of the Burning of Powder.

In choosing a test characteristic for the progressive burning of powder, the expression used must be such as would be determinable on the basis of geometric data for the ideal case, assuming that the powder mass is fully homogeneous.

At the same time the numerical value of this characteristic must be found exclusively from such bomb test data whose values at any given instant are considered reliable within pre-established limits.

When powder is burned in a bomb, we get a pressure curve as a function of time, and it may be assumed that the pressure at every given instant is known to be correct within the limits of accuracy of the recording device itself.

If it is assumed that the powder energy  $f$  and its density  $\delta$  are constant throughout the entire mass and that no cooling occurs through the walls of the bomb, i.e., if we make the usual assumption peculiar to ballistics, then, on the basis of the general pyrostatics formula, the pressure  $p$  at a given loading density is fully determined by the amount of the burned portion of charge  $\psi$  regardless of the powder shape and its rate of burning.

Indeed, the dependence of  $p$  on  $\psi$  is expressed by the formula

$$p - p_B = \frac{f \Delta \psi}{1 - \frac{\Delta}{\delta} - \Delta \psi \left( \alpha - \frac{1}{\delta} \right)},$$

into which time does not enter, and the pressure is determined by the burned portion of charge  $\psi$  when the other factors remain constant.

If, however, in addition to pressure its increase with relation to time must be known also, the magnitude of  $dp/dt$  will be determined by the velocity of gas formation  $d\psi/dt$  and by its variation with time.

The values of this magnitude are determined directly from test, because in measuring the curve the values of  $p$  are known at definite time intervals  $t$ , as are the values of  $\psi$  corresponding to these

values of  $p$ . If the intervals taken are sufficiently small, the values of the increment  $\Delta\psi$  can be found as the difference between two neighboring intervals, following which  $\Delta\psi/\Delta t$  can be found as well (limit -  $d\psi/dt$ ).

The value of  $d\psi/dt$  which, in the case of the geometric law of burning, is expressed by the formula  $\frac{d\psi}{dt} = \frac{S_1}{A_1} \frac{S}{S_1} u_1 p$ , depends on.

pressure. In order to compare various burning periods with respect to the rate of gas formation (increasing and decreasing rates) at constant pressure, as is usually done in the case of the geometric law, the obtained values  $d\psi/dt$  must be reduced to constant pressure, i.e., a comparison must be made of the values  $d\psi/dt : p = \frac{1}{p} \frac{d\psi}{dt}$ .

If the value of  $\frac{1}{p} \frac{d\psi}{dt}$  increases as burning progresses, the powder will burn progressively, if it decreases - the burning is regressive.

Henceforth we shall designate this magnitude by  $\Gamma$  (gamma):

$$\Gamma = \frac{1}{p} \frac{d\psi}{dt}.$$

It represents the specific rate of gas formation reduced to  $p = 1$ , which we shall hereafter call the intensity of gas formation.

Its variation during the burning process is characterized by the powder from the point of view of progressive burning, rather than by the shape of the grain alone. The dimensionality of  $\Gamma$ , which is

equal to  $\frac{1}{\frac{\text{kg}}{\text{dm}^2} \cdot \text{sec}}$ , is the inverse of the dimensionality of

pressure impulse.

F-TS-7327-RE

In the ideal case at constant pressure the value of  $\Gamma$  varies in proportion to the powder surface, as it does in the case of the geometric law of burning, and this value is therefore a characteristic of progressivity.

Actually, if ignition were to occur instantaneously along the entire area of the charge and the pressure during the entire process were to remain constant and equal to  $p_0$ , then a chemically homogeneous powder composition would burn according to the geometric law in parallel layers. In such a case the intensity of gas formation would vary in proportion to the change in area.

Indeed,

$$\frac{d\gamma}{dt} = \frac{S_1}{\Lambda_1} \frac{S}{S_1} u = \frac{S_1}{\Lambda_1} \frac{S}{S_1} u_1 p_0.$$

The magnitude of  $\Gamma$  will be represented in the following form:

$$\Gamma = \frac{1}{p_0} \frac{d\gamma}{dt} = \frac{S_1}{\Lambda_1} \frac{S}{S_1} u_1.$$

When the composition of the powder is homogeneous,  $u_1$  is constant and  $S_1/\Lambda_1$  is a constant; hence the variation of  $\Gamma$  will be proportional to the  $S/S_1$  ratio, i.e., the characteristic of the progressivity of burning will coincide with the powder grain characteristic.

Thus, as the test characteristic of the progressivity of burning, we can take the value  $\Gamma = \frac{1}{p} \frac{d\gamma}{dt}$  - the intensity of gas formation.

The value of  $\Gamma$  is found by the sectional analysis of the pressure test curve in a constant volume.

The function  $\Gamma$  enables us to evaluate the progressivity of the actual burning of powders of any shape and size, of both a homogeneous and heterogeneous mass.

The rate of gas formation in burning powder in a bomb can be evaluated by its actual law of burning even if the shape and dimensions of the powder are not known. The nature of the burned powder is determined by the values

$$\psi \text{ and } \frac{1}{p} \frac{d\psi}{dt}.$$

The law of burning expressed by the function  $\Gamma = \frac{1}{p} \frac{d\psi}{dt}$  and obtained by analyzing the pressure test curve  $p, t$ , wherein are reflected the peculiarities of the properties of actual powder and the deviations of its burning from that of an ideal powder, is called the experimental or physical law of burning.

Along with the  $\Gamma, \psi$  and  $\Gamma, t$  curves, the curve showing the pressure impulse variation  $\int_0^t p dt$  as a function of  $\psi$  also serves as a characteristic of actual powder burning.

These integral curves and their values will be discussed in detail later in the text.

The procedure for analyzing the  $p, t$  curve for determining  $\int p dt, \psi$  and  $\Gamma, \psi$  is illustrated in Table 13.

When computing  $\Delta$ , the mean value must be taken between the initial  $\Delta_0 = \frac{w}{W_0}$  and  $\Delta_K$  at the end of burning:

$$\Delta_K = \frac{\omega}{W_0 + s\xi},$$

where  $\xi$  - compression produced by the crusher;

$s$  - cross section of the piston.

The covolume effect of the igniter  $\alpha_B$  can be disregarded:

$$\Delta_{cp} = \frac{\Delta_0 + \Delta_K}{2} = \frac{\omega}{W_0 + s \frac{\xi}{2}}.$$

The  $\Gamma$ ,  $\psi$  and  $\Gamma$ ,  $t$  diagrams offer a visual interpretation of the change in the intensity of gas formation and enable one to analyze the processes occurring during ignition of the charge and during actual burning of the powder with all its peculiarities.

The diagrams in fig. 46, 47, 48 and 49 contain experimental  $p$ ,  $t$  curves as a function of time for tubular powders (fig. 46), strip powders (fig. 47), powders with 7 perforations (fig. 48) and Kisnensky's powder with 36 perforations (fig. 49), and also curves showing the variation of  $\Gamma$  as a function of  $t$ , where the corresponding  $\Gamma$  and  $p$  points lie on the same vertical.

For a constant value of  $u_1$ , the change of  $\Gamma = \frac{S_1}{\Lambda_1} u_1 \frac{S}{S_1}$  must proceed in proportion to the change of the geometric surface ratio  $S/S_1$ , i.e., in the case of strip and tubular powders  $\frac{S}{S_1}$  must be maximum at the start and undergo a very small decrease during burning; at the end, in the case of the geometric law of burning,  $S_K/S_1 \approx 0.90$ .

Nevertheless, the  $\Gamma$ ,  $t$  curves in fig. 46 and 47 are very peculiar in character: they start at some small value (pressure) and then proceed to ascend; after reaching the maximum at  $t \approx 0.0045$  (which corresponds to a pressure of 150-170 kg/cm<sup>2</sup>) the curve begins to descend, and after  $t = 0.0115$  for strip powder and 0.0135 for tubular powder the  $\Gamma$  curve drops abruptly to zero. On the  $p$ ,  $t$  curves this condition corresponds to the inflexion point  $p_1$ .

Table 13

6	7	8	9	10	11
$-\Sigma p_{cp} \cdot \Delta t \approx \int p dt$	$\beta = \frac{p - p_B}{p_m - p_B}$	$\psi(***)$	$\Delta \psi$	$\Gamma = \frac{\Delta \psi(**) }{\Delta I} = \frac{\Delta \psi}{p_{cp} \Delta I}$	$\psi_{cp}$
0	0	0	$\Delta \psi'$	$\Gamma' = \frac{\Delta \psi'}{\Delta I'}$	$\psi'_{cp}$
$-\Delta I'$	$\beta'$	$\psi'$	$\Delta \psi''$	$\Gamma'' = \frac{\Delta \psi''}{\Delta I''}$	$\psi''_{cp}$
$-I' + \Delta I''$	$\beta''$	$\psi''$	$\Delta \psi'''$	$\Gamma''' = \frac{\Delta \psi'''}{\Delta I'''}$	$\psi'''_{cp}$
$-I'' + \Delta I'''$	$\beta'''$	$\psi'''$	.	.	.
.	.	.	.	.	.
.	.	.	.	.	.
.	.	.	.	.	.
$K$	.	.	.	.	.
$-\sum (\Delta I)$	1	1	.	.	.
0					

increase curve for the purpose of calculating the powder characteristics, of the igniter is discarded and the analysis is started at pressure  $p_B$ .



Table 13

1	2	3	4	5	6	7
t	p(*)	$\Delta p$	$p_{cp}$	$p_{cp} \Delta t = \Delta I$	$I = \sum p_{cp} \cdot \Delta t \approx \int p dt$	$\beta = \frac{p - p_B}{p_m - p_B}$
0	$p_B$	$\Delta p'$	$p'_{cp}$	$\Delta I'$	0	0
t'	$p'$	$\Delta p''$	$p''_{cp}$	$\Delta I''$	$I' = \Delta I'$	$\beta'$
t''	$p''$	$\Delta p'''$	$p'''_{cp}$	$\Delta I'''$	$I'' = I' + \Delta I''$	$\beta''$
t'''	$p'''$	$\Delta p''''$	.	.	$I''' = I'' + \Delta I'''$	$\beta'''$
.	.	.	.	.	.	.
.	.	.	.	.	.	.
.	.	.	.	.	.	.
.	.	.	.	.	.	.
t <sub>K</sub>	$p_m$				$I_K = \sum_{0}^K (\Delta I)$	I

## Remarks.

(\*) When analyzing the pressure increase curve for the purpose of calculating the portion representing the burning of the igniter is discarded and the

(\*\*) When plotting the curve on the diagram, the values of  $\int p dt$  from the curve are plotted as a function of  $\psi$ , because both  $\int p dt$  and  $\psi$  relate to the same pressure. As regards the change in the rate of gas formation on the curve section representing the burning, hence its values are plotted as a function of the mean  $\psi$  characterizing the

(\*\*\*) When computing  $\psi$  by means of the tables, the entrant number is the number in steps of 0.01 from 0.86 to 0.97.

Table 13

6	7	8	9	10	11
$\sum p_{cp} \cdot \Delta t \approx \int p dt$	$\beta = \frac{p - p_B}{p_m - p_B}$	$\psi(***)$	$\Delta\psi$	$\Gamma = \frac{\Delta\psi(**)}{\Delta I} = \frac{\Delta\psi}{p_{cp} \Delta t}$	$\psi_{cp}$
0	0	0	$\Delta\psi'$	$\Gamma' = \frac{\Delta\psi'}{\Delta I'}$	$\psi'_{cp}$
$I' = \Delta I'$	$\beta'$	$\psi'$	$\Delta\psi''$	$\Gamma'' = \frac{\Delta\psi''}{\Delta I''}$	$\psi''_{cp}$
$I'' = I' + \Delta I''$	$\beta''$	$\psi''$	$\Delta\psi'''$	$\Gamma''' = \frac{\Delta\psi'''}{\Delta I'''}$	$\psi'''_{cp}$
$I''' = I'' + \Delta I'''$	$\beta'''$	$\psi'''$	.	.	.
.	.	.	.	.	.
.	.	.	.	.	.
.	.	.	.	.	.
.	.	.	.	.	.
$K$ $= \sum_{0} (\Delta I)$	I	I			

increase curve for the purpose of calculating the powder characteristics, of the igniter is discarded and the analysis is started at pressure  $p_B$ .

On the diagram, the values of  $\int p dt$  from column "6" are plotted as a function of pressure to the same pressure. As regards the value of  $\Gamma$ , it characterizes the mean value of the curve section representing the variation of  $\psi$  between  $\psi_i$  and  $\psi_{i+1}$ ;  $\Gamma$  is the mean value of the mean  $\psi$  characterizing the given section of the  $\Delta\psi$  variations.

In the tables, the entrant number is the parameter  $\beta = \frac{1 - \alpha \Delta}{1 - \Delta/\epsilon}$ , varying

$\Gamma$ ,  $t$  curves with many perforations deviate from the theoretical to an even greater degree (fig. 48 and 49).

In fig. 48 the maximum  $\Gamma$  obtains at  $t = 0.0095$  ( $p \approx 240$ ), the rise of the  $\Gamma$  curve being rather gradual and smooth up to the point of maximum. Upon passing the maximum, the curve drops slowly throughout the entire burning process up to  $t = 0.019$ ; this is followed by a sharper drop, which corresponds to the decomposition of the grain and the afterburning of the regressive products of decomposition.

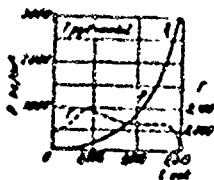


Fig. 46 -  $\Gamma$ ,  $t$  Characteristic for Tubular Powder.

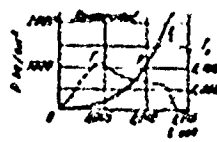


Fig. 47 -  $\Gamma$ ,  $t$  Characteristic for Strip Powder

1)  $p$  kg/cm<sup>2</sup>; 2) tubular; 3)  $t$  (sec). 1)  $p$  kg/cm<sup>2</sup>; 2) strip; 3)  $t$ (sec).

On fig. 49,  $\Gamma$  rises slowly at first, and at  $t = 0.0075$  ( $p = 120$ ) it proceeds to ascend very sharply; the ordinate increases almost two-fold and has a maximum at  $t = 0.009$  ( $p = 180$ ); after reaching the maximum the curve undergoes a continuous drop becoming more pronounced at  $t = 0.015$ , which corresponds to the instant the grain undergoes decomposition.

GRAPHIC NOT REPRODUCIBLE

# GRAPHIC NOT REPRODUCIBLE

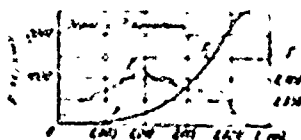


Fig. 48 -  $\Gamma$ , t Characteristic for a Grain with 7 Perforations

1)  $p$  kg/cm<sup>2</sup>; 2) grain with 7 perforations; 3)  $t$  (sec).

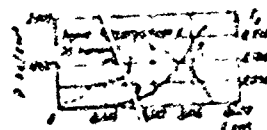


Fig. 49 -  $\Gamma$ , t Characteristic for Kisnensky's Grain with 36 Perforations.

1)  $p$  kg/cm<sup>2</sup>; 2) Kisnensky's grain with 36 perforations; 3)  $t$  (sec).

Thus during the process of burning from  $p \approx 200$  kg/cm<sup>2</sup> to the end, perforated grains burn with a seemingly decreasing surface area, whereas theoretically the area should continue to increase until decomposition occurs.

$\Gamma$ ,  $\psi$  curves. In order to obtain a more detailed comparison of the test data with theoretical data, the  $\Gamma$  curves are plotted as a function of the burned portion of the charge  $\psi$ , because if plotted as a function of time, when the pressure continuously increases and the process of burning is accelerated, the  $\Gamma$  curve becomes distorted in the direction of the abscissa ( $x$  - axis): the initial sections (of the curve) at low pressures are stretched, and those at higher pressures - at the end of burning - compressed.

The obtained curves of  $\Gamma$  plotted as a function of  $\psi$  are presented in the diagram of fig. 50-53, which diagrams also show theoretical

curves of  $\Gamma_T = \frac{S_1}{\Lambda_1} u_1 \frac{S}{S_1}$  when  $S/S_1$  varies according to the geometric

law of burning.

F-TS-7327-RE

The average value of  $u_1$  for pyroxylin powders is taken to be 0.075 mm/sec.

An analysis of experimental  $\Gamma, \psi$  curves for powders of simple shapes (fig. 50 and 51) will show that such curves consist of four distinct sections.

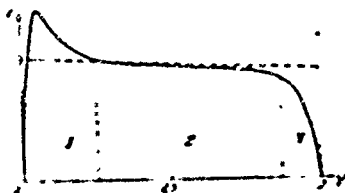


Fig. 50 -  $\Gamma, \psi$  Characteristic Curve for Tubular Powder.

Section I of the curve starts not at the maximum, as it should be in the case of instantaneous ignition, but, rather, increases from a small value to the maximum; the  $\Gamma$  maximum is obtained at  $\psi = 0.05 - 0.08$  and considerably exceeds the theoretical maximum.

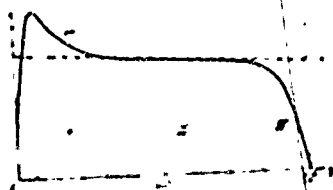


Fig. 51 -  $\Gamma, \psi$  Characteristic Curve for Strip Powder.

Section II -  $\Gamma$  drops from maximum to a point from which the curve follows a theoretical path - a section depicting accelerated burning; this section is confined between the limits of  $\psi = 0.05 - 0.08$  and

$\psi \approx 0.30$ .

F-TS-7327-RE

189

GRAPHIC NOT REPRODUCIBLE

Section III depicts normal burning which coincides with the geometric law;  $\psi$  varies from 0.30 to 0.85 - 0.90.

Section IV from  $\psi \approx 0.85-0.90$  to the end of burning. Here the experimental curve deviates from the theoretical downward and drops to zero at  $\psi = 1$ .

The  $\Gamma$ ,  $\psi$  curves for powders with narrow perforations (figs. 52 and 53) have even a larger number of deviations from the theoretical. Furthermore, the reduction of the ordinates of  $\Gamma$  corresponding to powder decomposition commences at  $\psi_{\text{son}} \approx 0.70-0.75$  and has no sharp angle point. Decomposition proceeds gradually because in practice the web thicknesses in a grain are not uniform, and a partial decomposition commences after the smallest thickness is burned. Increasingly thicker elements are gradually burned away and progressive burning occurs simultaneously with regressive burning of the products of decomposition.

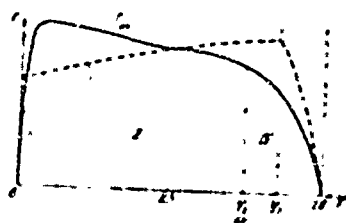


Fig. 52 -  $\Gamma$ ,  $\psi$  Characteristic Curve for a Grain with 7 Perforations.

# GRAPHIC NOT REPRODUCIBLE

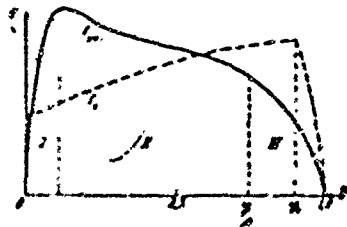


Fig. 53 -  $\Gamma, \psi$  Characteristic Curve for a Kisnemy Grain with 36 Perforations.

As a result, the transition from burning with an increasing surface to the afterburning of the products of decomposition is gradual rather than abrupt in character.

## CHAPTER 2 - BALLISTIC ANALYSIS OF THE ACTUAL BURNING OF POWDER

### 1. TESTS FOR INVESTIGATING THE IGNITION OF POWDER

#### A. Effect of the Size and Nature of the Igniter

##### a) Theoretical Data. .

We had derived above (fig. 50) a formula for determining the full time of burning when the powder is ignited instantaneously:

$$t_K = 2.303 \tau \log P_m / P_B$$

and shown that for a given loading density the time of burning decreases with the increase of the igniter pressure.

Calculations show that for  $\Delta \approx 0.20$  at  $P_m - P_B = 2000 \text{ kg/cm}^2$  and at  $P_B = 20; 40; 60$  and  $120 \text{ kg/cm}^2$ ,  $t_K$  varies within the following limits (Table 14).

Table 14

$P_B$	20	40	60	120
$t_K$ , sec	0.0140	0.0119	0.0107	0.0087
$\frac{t_K}{t_{K\ 120}}$	1.61	1.37	1.23	1.00

In this case the  $\Gamma$ ,  $t$  and  $\Gamma$ ,  $\psi$  curves (for strip powders) must start at the maximum and then descend slightly as the surface area of powder  $\delta$  decreases.

Hence, in the case of instantaneous ignition at  $\Delta \approx 0.20$ , if  $t_{K\ 120}$  is taken as the unit time at  $p = 120\text{ kg/cm}^2$ , the time of burning  $t_{K\ 20}$  will be increased by 61% if the igniter pressure is decreased to  $20\text{ kg/cm}^2$ .

Actual tests show however that the difference in the periods of burning at such igniter pressures is considerably greater.

#### b) Test Data.

Strip powder "CII" about 1 mm thick (1 x 18 x 40) was burned in a manometric bomb at  $\Delta = 0.20$  using batches of igniter material developing a pressure of  $p_B = 20, 40, 60$  and  $120\text{ kg/cm}^2$ .

The igniter used was dry powdered pyroxylin. Pressure was recorded by means of conical crushers. The test data are presented below in Table 15.



Table 15

$p_B$	20	40	60	120
$t_K$ , sec	0.0280	0.0160	0.0133	0.0090
$\frac{t_K}{t_K \text{ } \tau_{\text{eop}}}$	3.10	1.60	1.48	1.00
$t_K \text{ } 120$				
$t_K \text{ } \tau_{\text{eop}}$	0.0140	0.0119	0.0107	0.0087

Note:  $t_K \text{ } \tau_{\text{eop}} = t_K \text{ theoretical}$

A comparison of this data with the figures in the preceding table shows that the difference in the burning periods is considerably greater than the theoretical difference. Particularly great is the divergence between the test time  $t_K$  and the theoretical one when the igniter used was weak:  $p_B = 20 \text{ kg/cm}^2 \left( \frac{t_{K. \text{ on}}}{t_K \text{ } \tau_{\text{eop}}} - 2 \right)$ ; (\*) this divergence becomes smaller as  $p_B$  increases and practically disappears at  $p_B = 120 \text{ kg/cm}^2$  (ratio  $t_{K. \text{ on}} : t_K \text{ } \tau_{\text{eop}} \approx 1$ ).

Analogous relationships were obtained with other samples (igniter materials).

Inasmuch as the  $p$ ,  $t$  curves showed no sharp changes along their ascent,  $\Gamma$ ,  $t$  and  $\Gamma$ ,  $\psi$  curves obtained from the analysis of corresponding  $p$ ,  $t$  curves from the start to the end of burning were utilized for the analysis of the processes of ignition.

(\*) Subscript "on" stands for the word "test," subscript "eop" stands for the word theoretical - translator.

In order to determine experimentally, by the aid of function  $\Gamma$ , the process of ignition - whether instantaneous or gradual, it was necessary to determine the presence of the following conditions:

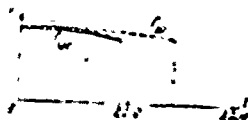


Fig. 54 - Theoretical  $\Gamma$ ,  $t$  Curves at Different Values of  $p_B$ .

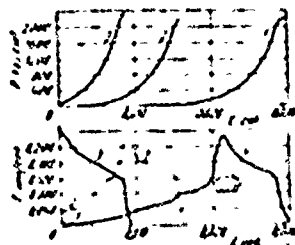


Fig. 55 - Experimental  $p_1 t$  and  $\Gamma_1 t$  Curves at Different Igniter Pressures.

a)  $\Gamma$  mm/sec; b)  $P$  kg/cm<sup>2</sup>; c)  $t$  (sec).

1. If the ignition is instantaneous, the curve of  $\Gamma$  variation for strip and tubular powders burning with a decreasing surface must start at the maximum.

2. If the ignition is instantaneous, the shape of the  $\Gamma$  curve must not depend on the size of the igniter, because after the entire surface is ignited its change must follow one and the same law.

GRAPHIC NOT REPRODUCIBLE

The theoretical  $\Gamma$ ,  $t$  curves must have the form shown in fig. 54.

The above diagram (fig. 55) illustrates the experimental  $p$ ,  $t$  curves obtained from the instant the powder became ignited; the  $\Gamma$ ,  $t$  curves corresponding to them are plotted to the same scale of time  $t$  under the corresponding  $p$ ,  $t$  curves. With the smallest igniter  $\omega_B$ , developing a pressure of about  $20 \text{ kg/cm}^2$ , the  $\Gamma$ ,  $t$  curve starts a very short distance above the origin and has a very long and gradually ascending section gradually changing to a steep slope, following which  $\Gamma$  maximum is reached (at  $p = \text{about } 225 \text{ kg/cm}^2$ ); this is followed by a rather sharp descent and, finally, by a very sharp drop at the end of the process. The growth of the ordinates of the curve at the start of burning corresponds to an increase of the burning area of the powder when its ignition proceeds gradually (curve 1).

When the igniter is increased by weight ( $2\omega_B$  - curve 2) the starting ordinate of  $\Gamma$  increases, i.e., a larger area becomes enveloped at the same time, the length of the slowly ascending section of the curve becomes smaller. Otherwise the  $\Gamma$ ,  $t$  curves practically remain unchanged; they seem to tend to shift to the left towards the origin of the coordinates, whereby the maximum value of  $\Gamma$  is the same as in the first case, at pressure  $p = 225\text{--}250 \text{ kg/cm}^2$ . When the igniter is maximum  $6\omega_B$  ( $p_B = 127 \text{ kg/cm}^2$  - curve 3), the curve  $\Gamma$  starts almost at the maximum point.

These results indicate that ignition at pressures of 20 to  $60 \text{ kg/cm}^2$  does not proceed instantaneously, and is the slower, the lower the igniter pressure - and only at  $p_B \approx 125 \text{ kg/cm}^2$  is the ignition almost instantaneous.

Inasmuch as in guns the pressure developed by the igniter is between 10 and 40 kg/cm<sup>2</sup>, the ignition will not be instantaneous. This is confirmed by the hangfire phenomenon.

## GRAPHIC NOT REPRODUCIBLE

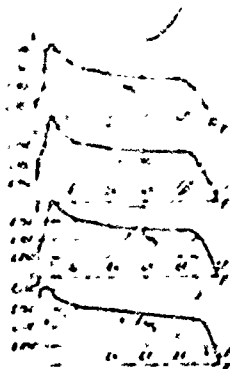


Fig. 56 - Experimental  $\Gamma$ ,  $\psi$  Curves at Different Igniter Pressures.

If we plot on a diagram the same curves of  $\Gamma$  as a function of  $\psi$  to facilitate their comparison with curves of the variation of  $S/S_1$  as a function of  $\psi$ , we shall obtain a diagram as illustrated in fig. 56.

When plotted as a function of  $\psi$ , the general appearance of the  $\Gamma$ ,  $\psi$  curves changes, they resemble more curves  $S/S_1$ ,  $\psi$ , but with certain deviations. As the value of  $\omega_B$  increases, the maximum of  $\Gamma$  shifts from  $\psi \approx 0.10$  towards the origin of the coordinates, and the descent of the curve becomes increasingly sharper whereby its end shifts from  $\psi_1 = 0.85$  to  $\psi = 1$ .

This indicates that during the interval it takes for the entire surface of a strip powder charge to become ignited, about 5-10% of the entire charge will be burned.

The larger the igniter, the more rapidly will the flame envelope the surface of the powder and the later will the start of decomposition and afterburning of the strip occur.

In the tests mentioned, the point of inflexion, whose position on the pressure curve serves to determine the exponent  $\beta$  as a "function of the shape," varied as follows when the igniter changed from  $\omega_B$  to  $6\omega_B$ :  $\psi_i = 0.85; 0.875; 0.90; 0.92$ .

Therefore, the smaller the igniter, the longer will it take for the entire surface of the powder to become ignited, and the more heterogeneous will be the strip in thickness; this results in a curve in which the point of inflexion occurs at an earlier stage.

If the exponent  $\beta$  as a "function of shape" is calculated by the formula

$$\beta = \frac{p_m - p_i}{p_i} = \frac{p_m}{p_i} - 1 \approx \frac{1}{\psi_i} - 1,$$

then, as  $p_B$  varies from 20 to 120 kg/cm<sup>2</sup>, we will obtain, respectively:

$$\beta = 0.18; 0.14; 0.11; 0.09.$$

The above deductions fully confirm in actual tests that the noninstantaneous ignition must affect the subsequent burning of the powder in a specific manner, increasing the value of  $\beta$  and making the burning process more regressive (transition from curve 4 to curve 1 in fig. 56). A comparison of the  $\tau, \psi$  curves in fig. 56 with

the "shape function" graph for strip powders at  $\beta = 0.2$  (fig. 45), shows an almost full coincidence of both the middle and terminal sections of these curves. However, the initial portions of the curves representing the first third of the process considerably differ from the theoretical form. They include: 1) ascending sections not present in the  $\delta = (1 - \psi)^\beta$  curve; 2) "ballooning" or a rather sharp increase of the ordinate compared with the Charbonier curve within the limits of  $\psi \approx 0.10$  and  $\psi \approx 0.30$ .

"Ballooning," i.e., the sharp increase of the ordinate, represents an abnormal increase in the rate of gas formation at the start of burning, which ascent gradually levels off and coincides with the theoretical curve in the second third of the process; this phenomenon was not known to exist earlier.

Thus, it is proven by the aid of  $\Gamma$ ,  $t$  and  $\Gamma$ ,  $\psi$  curves, that the ascending first section of the curve from  $\Gamma$  to  $\Gamma_{\max}$  at the start of burning represents a process of gradual ignition and the increase of the burning area of the powder due to noninstantaneous ignition. Ignition may be considered practically instantaneous only at  $p_B = 120-150 \text{ kg/cm}^2$ .

If batches of pyroxyline and granulated black powder (of the rifle type) are prepared in such a manner as to produce the same pressure  $p_B$ , the ignition process will be more vigorous in the case of black powder, so that the latter will not succeed in getting fully burned by the time the basic charge of pyroxyline powder begins to burn (sic).

This is in full accord with the nature of the igniters. Whereas the products of decomposition of pyroxylin constitute a high temperature gas mixture, in the case of black powder these products also contain incandescent hard particles. The impacts of many such incandescent hard particles help to ignite the surface of the powder more rapidly than do the impacts of gas molecules.

## 2. THE NATURE OF "BALLOONING."

"Ballooning" is a term designating a condition where the test curve of progressivity  $\Gamma$  exceeds the theoretical curve (Section II). This phenomenon is observed in powders with a volatile solvent, and is peculiar to a greater extent to thick powders than to thin ones, and to nitroglycerine powders than to pyroxylin ones. Powders with a solid solution produce practically no ballooning, - their burning approaches the geometric law more closely.

The cause of ballooning can be discovered by choosing powders of the same shape and size but of different properties.

In such a case the exposed grain area and the change in the surface area will be the same in both powders, and the difference in the values of  $\Gamma_{on}$  and  $\Gamma_{reop}$  (i.e.,  $\Gamma_{test}$  and  $\Gamma_{theor.}$  - respectively) can be obtained only because of the difference in the burning rate  $u_1$ , because

$$\Gamma = \frac{S_1}{A_1} \cdot \frac{S}{S_1} u_1.$$

The shape of the  $\Gamma$ ,  $\psi$  curves obtained by burning two samples of tubular powder of the same size is shown in fig. 57; curve 1

corresponds to a powder with a volatile solvent, and curve 2 to a powder with a solid solvent (trotyl + pyroxylin).

The first one produces considerable ballooning, and in the second there is practically no ballooning at all. The difference between the ordinates of these two curves is explained by the difference in their rate of burning because of the heterogeneous mass of the first sample produced by wetting the powder in water for the purpose of removing the excess of volatiles. When wetted, the powder becomes more porous on the outside and this tends to increase the rate of burning of the outer layers; as the burning layer is shifted inwardly, the rate of burning slows down. The inner portion of the powder layer is usually not affected by the wetting operation and therefore burns at a normal rate.

A somewhat higher rate of burning  $u_1$  of the outer layers of powder with a solid solvent, homogeneous throughout its mass, can be partly explained by the more penetrating and intensive heating of the boundary layers of the powder at low pressures, while burning process proceeds with a relatively small absolute speed, and by reduced heating - as the burning process proceeds with a higher absolute rate of speed when the pressure increases to above 500 kg/cm<sup>2</sup>. The layers of powder directly in contact with the burning surface will, in this case, become less heated and to a smaller depth, as a result of which the value of  $u_1$ , and with it the value of  $\Gamma$ , will become decreased.

This explanation suggested by the author in 1937 [5] is now substantiated in the theory of powder burning developed by Prof. Ya. B.



Zeldovich, although the cause of ballooning has not been fully established as yet.

In any case, ballooning is the accelerated burning of the outer powder layers, occurring at relatively low pressures and, mainly, in the case of powders with volatile solvents.

The thicker the powder and the smaller its mean burning rate, the higher will be its relative degree of ballooning.

Ballooning becomes nil when the pressure is increased because of accelerated burning.

An analysis of the experimental  $\Gamma$ ,  $\psi$  curves made it possible to establish the following empirical relationship between the burning rate  $u_1$  and the depth of the layer:

$$u_1 = u_1' e^{-a\sqrt{z}},$$

where  $u_1'$  - the burning rate of the outer layer ( $u_1'$  for almost all pyroxylin powders is of the same order - 0.0000120 to 0.0000125 dm/sec : kg/dm<sup>2</sup>);

$z$  - relative thickness of the burned layer, equal to  $\psi$  for tubular powder and approaches  $\psi$  for strip powder;

$a$  - coefficient characterizing the drop in the burning rate and determined from the  $\Gamma$ ,  $\psi$  curve.

# GRAPHIC NOT REPRODUCIBLE



Fig. 57 - Intensity of Gas Formation in Powders of Different Properties.

This formula is valid for values of  $z$  from 0 to  $z_c \approx 0.3$ , and the magnitude of  $a$  can be found by the following formula:

$$a = \frac{\ln \frac{u_1'}{u_1}}{\sqrt{z_c}} = \frac{2.303}{\sqrt{z_c}} \log \frac{u_1'}{u_1},$$

where  $u_1$  is the constant burning rate of internal layers after  $z = z_c$ .

The curves in fig. 58 show the variation of rate  $u_1$  from one layer to another in the case of "CN" powder 1 mm thick and "Б<sub>14</sub>" powder 6 mm thick; for the first powder  $u_1' = 0.04120$ ,  $u_1 = 0.0575$  and  $a = 0.858$ ; for the second powder  $u_1' = 0.04125$ ,  $u_1 = 0.0560$  and  $a = 1.34$ .

The "Б<sub>14</sub>" powder has a considerably higher content of volatiles, and hence its average burning rate  $u_1 = 0.0560$ ; the content of volatiles in "CN" powder is smaller and  $u_1 = 0.0575$ . However, inas-

much as thick powders are subjected to longer periods of wetting, the burning rate of their outer layers is even higher than in the "CN" powder ( $0.0_4125$  and  $0.0_4120$ ).

## GRAPHIC NOT REPRODUCIBLE



Fig. 58 - Change of  $u_1$  During Burning.

The above formula shows that the burning rate of powders with a volatile solvent is not constant, as was assumed previously, but variable, being higher in the outer layers than in the inner ones. As a result, the effective burning of powder is more regressive than that assumed on the basis of a changing burning area  $S$  only, while considering the rate  $u_1$  constant.

If the deviation of burning from the geometric law is due to the difference in the thickness of the elements of the charge and to the heterogeneity of the powder mass, would it be possible to obtain a  $\rho, \psi$  curve without ballooning? Is it possible to realize the geometric law of burning in actual practice? Well, the above is possible by observing certain conditions.

# GRAPHIC NOT REPRODUCIBLE

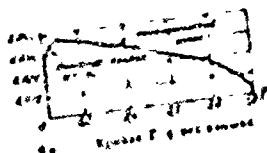


Fig. 59 -  $\Gamma, \psi$  Curve without Ballooning.

1) Test curve; 2) geometric law.

A solid cylindrical powder rod without a solvent (the mass is homogeneous) 7.5 mm in diameter by 42 mm long with rounded (spherical) ends, was fastened along the axis of a 21.5 cm<sup>3</sup> bomb by means of a frame made of thin copper wire. This arrangement facilitated ignition, and all the burning surfaces were subjected to identical conditions as regards the freedom of gas separation.

The weight of the igniter was such as would develop a pressure  $p_B = 160 \text{ kg/cm}^2$ , and insure instantaneous ignition.

Figure 59 contains an experimental  $\Gamma, \psi$  curve and its corresponding curve of the geometric law of burning at  $u_1 = 0.069 \text{ mm/sec}$ .

According to this diagram, no ballooning is observed on the test curve; the latter almost fully coincides with the theoretical curve upon reaching a maximum.

This shows that a powder which is entirely homogeneous in all its layers and is subjected to identical conditions as regards the freedom of gas separation from its surface elements, burns according to the geometric law.

A powder with a volatile solvent, whose burning rate varies from layer to layer deviates from the geometric law.

Furthermore, it is impossible to distribute a charge in such a manner where all the surfaces would be placed under identical conditions as regards freedom of gas separation, and to obtain a condition where the deviation from the geometric law would always be the greater, the greater is the difference in the conditions of burning at different portions of the charge.

### 3. THE POINT OF INFLEXION ON THE PRESSURE CURVE.

When deriving the theoretical relationship between pressure increase and time, it was shown that in the case of tubular and strip powders in which the burning area varies little, the rate of pressure increase must grow continuously and have a maximum value at the end of burning. Indeed, in the expression

$$\frac{dp}{dt} = \frac{f\Delta}{1 - \alpha\Delta} \frac{u_1}{e_1} \times \frac{S}{S_1} p \quad (49)$$

the value of  $S/S_1 \approx \text{const}$ , and  $p$  grows continuously.

At the same time, the many tests conducted by various investigators show that when tubular and strip powders are burned in a bomb, an inflexion point invariably occurs on the  $p, t$  curves, following which  $dp/dt$  decreases and approaches zero, and the curve takes on a "beak-like" shape.

Charbonier had determined the exponent  $\beta$  from test from the position of the inflexion point in his suggested expression for the "shape functions."

Some of the authors were of the opinion that the hook in the curve is the result of the crusher's "setting" after the end of burning by the inertia of the small piston, and does not depend on the law of powder burning.

The analysis of formula (49) indicates that in order to obtain the deflection point ( $dp/dt = \text{const}$ ), it is necessary to maintain the condition  $S \cdot p = \text{const}$ , and inasmuch as the gas pressure in the bomb undergoes a continuous increase, the burning powder surface must decrease at the point of inflexion ( $S = \text{const}/p$ ).

If, however, the reduction of the surface area proceeds faster than the pressure increase, then  $Sp$  and  $dp/dt$  will decrease in value, and the convex side of the  $p, t$  curve will be directed upwards.

Such curves are observed before the end of burning in the case of powders with 7 perforations, whose surface area rapidly decreases after decomposition.

It can be shown by test that the position of the point of inflexion, when burning strip powders, depends on the degree of homogeneity of the thickness of the plates making up the charge. By carefully selecting the proper strip thickness and arranging them in such a manner that the igniter gases would immediately envelope their entire surface, and using a strong igniter in order to obtain a simultaneous and instantaneous ignition, a  $p, t$  curve can be obtained with practically no inflexion at all, or, at any rate, a curve without a "beak."

Contrariwise, if the charge is intentionally made up of powder strips of a given grade but of varying thickness, the point of inflexion can be made to appear considerably earlier than usual [5]

Moreover, by making up a charge of strips of different grades of powder, we had succeeded in converting the  $p, t$  curve into a rectilinear curve along most of its length, i.e., create what would appear a whole series of inflexion points.

The table below contains some of the data obtained by M.E. Serebriakov in his tests, in which he attempted to determine the reasons for the appearance of an inflexion point  $\Delta = 0.20$ ; powder-Japanese strip, "CΠ"; igniter - dry pyroxylin].

In test No. 1 the charge was made up of strips, considerably varying in thickness; a weak igniter was used.

In test No. 2 the charge was made up of strips of uniform thickness, using the same igniter.

In test No. 3 the charge was the same as in test No. 2; a strong igniter was used.

The following was determined in all of these tests.  $p_i$  and  $\psi_i$  at the point of inflexion, powder burning time  $t_K$  and exponent  $\beta$ .

Table 16

$$W_0 = 78.5 \text{ cm}^3$$

test No.	$2e_1$ , mm	$p_B$ , kg/cm <sup>2</sup>	$\Delta = \frac{\omega + \omega_B}{W_0}$	$p_m$ kg/cm <sup>2</sup>	$p_1$ kg/cm <sup>2</sup>	$\left(\frac{dp}{dt}\right)_{\max}$ T/cm <sup>2</sup> /sec	$\psi_1$	$t_K$ sec	$\beta$
1	0.92-1.07	20	0.201	2115	1717	428	0.82	0.0355	0.230
2	1.00-1.01	20	0.201	2150	1950	480	0.92	0.0348	0.103
3	0.98-1.00	125	0.211	2310	2190	540	0.95	0.0084	0.055

Curves  $p$ ,  $t - \Gamma$ ,  $t$  and  $\Gamma$ ,  $\psi$  are shown in fig. 60-61.

The obtained results offer a very clear graphic description of these tests.

In test No. 1 the pressure curve past the point of inflexion has a fairly long "beak," and the transition from the point of inflexion to the end of the curve is smooth ( $\Delta t = 0.0030$  sec). No smooth transition after  $p_1$  occurs in test No. 2; there is a sharp break in the curve and the "beak" is considerably shorter ( $\Delta t = 0.0013$  sec).

In test No. 3 ignition occurs instantaneously, the uniformity of the thicknesses is retained, the point of inflexion shifts to the very end of burning,  $(dp/dt)_{\max}$  increases in value, and the "beak" is totally absent on the  $p$ ,  $t$  curve; the curve terminates at an angle approaching the maximum ( $\Delta t < 0.0005$  sec). No "aftercompression" of the crusher was noted in this test.



# GRAPHIC NOT REPRODUCIBLE

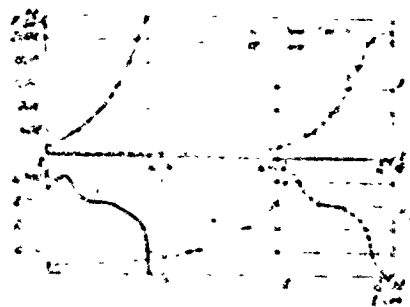


Fig. 60 -  $p$ ,  $t$  and  $\rho$ ,  $t$  Curves at Different Values of  $p_B$  and  $2e_1$ .

a)  $p$ ,  $\text{kg/cm}^2$ ; b)  $t$  (sec); 1) ... 1.07 mm "CП" strip; 3) ... 1.00 mm "CП" strip.

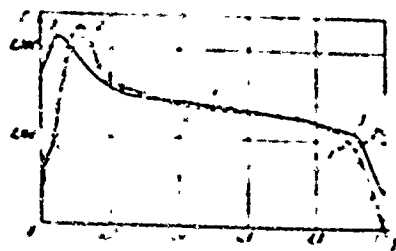


Fig. 61 -  $\rho$ ,  $\psi$  Curves at Different Values of  $p_B$  and  $2e_1$ .

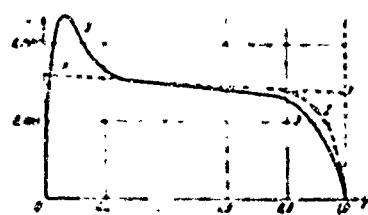


Fig. 62 -  $\rho$ ,  $\psi$  Curves at End of Burning of Strips of Different Thicknesses.

GRAPHIC NOT REPRODUCIBLE

Thus, the appearance of an inflexion point is linked with the sharp surface area decrease during burning of powder.

Its position, in the case of strip and tubular powders, depends on the uniformity of the thickness of the strips or tubes at the end of burning.

By choosing the proper conditions of ignition  $p_B$  and thickness of the strips, the position of the inflexion point on the pressure curve can be varied widely.

This point always occurs in the case of powders of nonuniform thickness or perforated powders, in which the burning surface area after decomposition undergoes a sharp decrease and tends towards zero.

#### 4. REASONS LEADING TO A LOWERED INTENSITY OF GAS FORMATION IN THE LAST STAGE OF BURNING

In the case of regressive powders, the experimental  $\Gamma, \psi$  curves in their mid-section between  $\psi = 0.3$  and  $\psi = 0.8-0.9$  almost coincide with the theoretical curves; beyond  $\psi = 0.8-0.9$  the ordinate of the curve begins to drop rapidly and tends towards zero at the end of burning whe.  $\psi = 1$ .

The reason for this drop lies in the nonuniformity of the plates making up the charge. The thinner the plate, the sooner will it burn. At the end of burning the surface area of such a plate undergoes a specific amount of reduction and this causes a decrease of the

function  $\Gamma = \frac{S_1}{\Delta_1} \frac{S}{S_1} u_1$ . The greater the nonuniformity of the charge

in thickness, the earlier will the condition of lowered intensity of

gas formation occur. Furthermore, even an individual strip is usually nonuniform in thickness along its entire width, so that after it is pressed during drying the contraction of the strip is not uniform and the latter acquires a slightly lenticular cross section: it is thicker in the middle than at the ends.

A similar and even greater variation can occur in the web thickness of tubular powder as a result of a nonconcentric perforation. The resulting noninstantaneous ignition causes further impairment of the initial plate dimensions and this advances the time at which the lowered intensity of gas formation at the end of burning occurs. This was shown in  $\Gamma$ ,  $\psi$  curves obtained in tests using igniters of different pressures, and also in fig. 61.

The results of calculating the change in the value of  $\frac{S}{A_1} u_1$ , for a charge consisting of plates of strip powder "C/F" varying in thickness from 0.92 to 1.17 mm and tested in a manometric bomb, are presented below.

In order to simplify such calculations, the plates were split up into 6 groups according to thickness; the relative number of plates of the two middle groups taken was greater than of the remaining groups, namely, 0.20 instead of 0.15%.

Theoretically, for a powder of uniform thickness, the ratio (exposure)  $S/A_1$  must vary during burning from 2.07 to 1.76  $\text{mm}^2/\text{mm}^3$ , and function  $\Gamma$  - from 0.160 to 0.136.

$$\frac{1}{\frac{\text{kg}}{\text{cm}^2} \text{ sec}} \text{ at } u_1 = 0.0775 \frac{\text{mm}}{\text{sec}} : \frac{\text{kg}}{\text{cm}^2} .$$

The following table gives the variation of  $S/\Lambda_1$  and  $\Gamma$  as a function of  $\psi$  during the burning of the individual plate groups [47].

Table 17

Group No.	1	2	3	4	5	6	Remarks
Plate thickness $2e_1$ in mm	0.92	0.97	1.02	1.07	1.12	1.17	$2e_1 \text{ cp} = 1.05 \text{ mm}$
Relative number of such plates in a charge	0.15	0.15	0.20	0.20	0.15	0.15	
$\psi_i$	0.894	0.931	0.961	0.982	0.994	1.000	
$\frac{S_1}{\Lambda_1}$	1.526	1.250	0.837	0.530	0.263	0	$\Gamma_0 \text{ cp} = 0.160$
$\Gamma_1 = \frac{S_1}{\Lambda_1} u_1$	0.118	0.097	0.069	0.041	0.020	0	$\Gamma_1 \text{ cp} = 0.136$

On the diagram in fig. 62, curve 1 corresponds to the theoretical variation of  $\Gamma$  for powders of average thickness; the descending portion 2 of the  $\Gamma_{\text{reop}}$  curve is obtained on the basis of the above table; this diagram also includes curve 3 of the test curve  $\Gamma$  obtained on the basis of a bomb test. A comparison of the theoretical and test  $\Gamma$  curves shows that their behavior both at the mid-section and at the end of burning is similar. The fact that curve 3 begins to drop ahead of curve 2 is explained by the use of a weak igniter in the test, and by the fact that the noninstantaneous ignition leads to an increased thickness variation.

## Conclusions

The above investigations clarify the reasons for the deviation of powder grains of plain shape from the geometric law of burning (Sections I, II, and IV in fig. 50).

The rapidly increasing section of the  $\Gamma, \psi$  curve at the start of burning constitutes a process of gradual ignition; a practically instantaneous ignition and the start of the curve directly from the maximum point is secured by the use of a high pressure igniter  $p_B = 120-150 \text{ kg/cm}^2$ .

"Ballooning" is the accelerated burning of powders at low pressures and in the presence of layers of nonuniform thickness, occurring as a result of technological processes (wetting) and excessive heating of the powder at low rates of burning.

The point of inflexion on the  $p, t$  curve and the corresponding rapid decrease of the intensity of gas formation shortly before the end of burning are due to the nonsimultaneous burning of the elements of the charge of varying thicknesses. The smaller the igniter, the greater will be the variation in the thickness of the powder, the earlier will the inflexion point occur, and the more rapid will be the drop in the intensity of gas formation. By choosing charge elements of the proper thickness and a very weak igniter, a condition can be obtained whereby the burning of the powder at the end would proceed without a sharp drop in the intensity of gas formation, and a  $p, t$  curve can be obtained without a point of inflexion.

## 5. BALLISTIC ANALYSIS

### A. The Application of $\rho$ , $\psi$ Curves to the Analysis of Burning of Flegmatized Powders

The powder must be flegmatized in order to make it a progressive powder, i.e., a substance tending to slow down the burning of the outer layers must be added to the powder mass. The distribution of the flegmatizer in the powder must be irregular - its concentration must be maximum in the outer layers and gradually diminish towards the center of the grain. Therefore, the burning rate  $u_1$  at  $p = 1 \text{ kg/cm}^2$ , which depends on the nature of the powder, must vary from a minimum in the outer layers to a maximum inside the grain. Progressive burning is thus obtained by changing the composition of the powder mass rather than from the shape of the powder.

Under actual factory conditions flegmatization may be inadequate or excessive, whereby the flegmatizer penetrates the full powder thickness and makes it slow burning rather than progressive in character.

It is of importance therefore to determine the depth of the flegmatizer's penetration, its distribution in the powder, and its effect on the burning rate  $u_1$ .

Usually the penetration of the flegmatizer is determined by coloring the flegmatizer solution with fuchsin (magenta red), and after flegmatization and drying the grain is cut and examined under a microscope.

This method is not very accurate however, because the penetrating properties of fuchsin and the flegmatizer may be different. The microscope enables one to determine the depth of penetration of fuchsin; it does not, however, permit one to determine the degree of distribution of the substance in the powder.

However, bomb tests and their analysis by means of the  $\Gamma$  function make it quite easy to obtain an accurate evaluation of the distribution of the flegmatizer throughout the mass of the powder.

Indeed, if we were to test in a bomb at a given loading density ordinary powder and then a flegmatized powder, and plot curves of the change of  $\Gamma$  as a function of  $\psi$ , the difference between these curves would be an appreciable one; this can be seen in fig. 63, which shows the test results obtained with powders with 7 perforations before and after flegmatization.

Whereas the nonflegmatized powder (curve 1) has "ballooning" present on the  $\Gamma, \psi$  curve and then drops to  $\psi = 0.50$ , flegmatized powder (curve 2) produces no ballooning, the ordinates of the curve move upward, and burning is progressive from the start up to  $\psi \approx 0.50$ ; thereafter the  $\Gamma, \psi$  curves almost coincide. Therefore, the effect of flegmatization is felt until half of the grain is burned, following which it is terminated. The above makes it possible to calculate the depth to which the flegmatizer has penetrated.

Inasmuch as in both cases the powder grains were of the same shape and dimensions, it may be assumed that the change of  $S/\Lambda_1$  with respect to  $\psi$  is the same in both cases. Hence the ratio of the ordinates  $\Gamma_2/\Gamma_1$  gives the ratio between the elementary burning rates at a given instant.

$$\frac{\Gamma_2}{\Gamma_1} = \frac{\left( \frac{S}{\Lambda_1} u_1 \right)_2}{\left( \frac{S}{\Lambda_1} u_1 \right)_1} = \frac{(u_1)_2}{(u_1)_1};$$

upon determining the value of this ratio for successive values of  $\psi$ , a curve can be constructed showing the relative variation of the elementary burning rate, which depends on the distribution of the flegmatizer in the powder mass.

An example of a curve of this type is shown in fig. 64.



Fig. 63 -  $\Gamma, \psi$  Curves for a Powder Before and After Flegmatization.

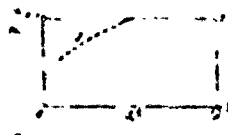


Fig. 64 - Change of Burning Rate  $u_1$  in a Flegmatized Powder.

The distribution of the flegmatizer in the powder is not uniform and becomes smaller as the depth of penetration is increased: this is indicated by the minimum value of the burning rate at the start and by the fact that the rate increases according to the law up to  $\psi = 0.50$ . Thereafter, the relative burning rate becomes equal to unity, i.e., the burning rates of the powders become the same. This indicates that the flegmatizer did not penetrate beyond  $\psi = 0.50$  and its corresponding thickness.

GRAPHIC NOT REPRODUCIBLE



Thus flegmatization serves to reduce the intensity of gas formation during the first half of the process. This permits increasing the charge in firing without exceeding the maximum pressure and to obtain a higher shell discharge velocity. But inasmuch as flegmatization usually lowers the powder energy  $f$ , in addition to the burning rate  $u_1$ , a portion of the increased charge is utilized for the purpose of maintaining the shell velocity which would have been obtained with nonflegmatized powder.

Inasmuch as the burning rate of powders containing uniformly distributed quantities of the flegmatizer can be determined from bomb tests, the variation of the flegmatizer concentration between the powder layers can be determined by the change in the burning rate of powders with different percentage contents of the flegmatizer material.

If the duration of the flegmatization process is overly long, a powder can be obtained in which the distribution of the flegmatizer is practically uniform throughout its entire thickness, and hence the burning of the powder will be slow but not progressive.

#### B. The Peculiar Burning Characteristics of Nitro-glycerine Powders

Analysis by means of the  $\Gamma$  function had shown that English tubular cordite, notwithstanding its regressive shape, gives a somewhat increased value of  $\Gamma$ , after  $\psi \approx 0.3$ , i.e., its burning is progressive.

It has been established by means of special tests, that a  $\Gamma, \psi$  curve constructed for freshly manufactured cordite does not differ in anyway from an ordinary  $\Gamma, \psi$  curve for tubular pyroxylin powder (curve 1-1-1 in fig. 65), after the excess of the solvent (acetone) is removed.

But if the "life" of such a powder is shortened by placing it in a thermostat at  $t = 50^{\circ}\text{C}$ , its energy will be lowered after a while and the  $\Gamma, \psi$  curve, following ballooning and a descent, will begin to ascend again from  $\psi \approx 0.3$  to  $\psi = 0.9$  (curve 2-2). Thereafter, its drop to zero will proceed more sharply, similarly to pyroxylin powders during the end burning of the thicker elements.

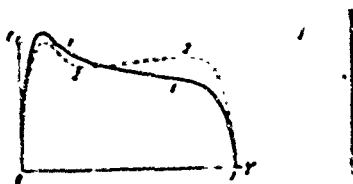


Fig. 65 -  $\Gamma, \psi$  Curves for Nitroglycerine Powder.

The fact that the energy  $f$  has decreased indicates that a portion of the nitroglycerin had evaporated through the outer surface of the powder. The nitroglycerine remaining in the layers close to the surface had shifted onto the surface causing ballooning during burning. This in turn had caused a redistribution of the nitroglycerin in the neighboring layers. Inasmuch as the rate of burning depends on the nitroglycerin content in the given layer, the rate should increase in the presence of such a nonuniform distribution as the

GRAPHIC NOT REPRODUCIBLE

burning process penetrates the grain in depth. And since  $\Gamma_T = \frac{S_1}{A_1} \frac{S}{S_1} u_1$ ,  $\Gamma$  increases because of the increase of  $u_1$ , and the burning of the powder becomes progressive. Therefore the burning characteristic of cordite can change depending upon its "age" and the conditions for its storing, and this change can be easily disclosed by using the test function  $\Gamma$  as the analyzer.

### CHAPTER 3 - BURNING PROPERTIES OF POWDERS WITH NARROW PERFORATIONS

It was shown above that test curves  $\Gamma, \psi$  of the progressivity of burning of powders with many narrow perforations deviate from the geometric law considerably more than do the curves of powders with grains of simple shapes (strip, short tube). These deviations are the greater, the longer the perforations, and, hence, the longer the powder grain itself.

The least understood phenomenon from the standpoint of the geometric law of burning are the regressive portions of the  $\Gamma, \psi$  curves in the case of perforated powders, whose surface area, theoretically, must undergo a continuous increase until the grain is decomposed.

If we consider such a change of the value of  $\Gamma$  from the standpoint of surface variation in a grain during burning, we get the impression that the grain becomes decomposed into separate parts in the form of rods after it is ignited, whose surface changes regressively. Such a decomposition of a grain during the initial stage of burning can occur for the reason that the gases formed inside

narrow and long perforations do not succeed in fully escaping from the perforations, thus creating a higher pressure which serves to accelerate burning. This pressure becomes so high that the walls of the powder collapse and the grain disintegrates, following which the burning of the powder becomes regressive.

Such an explanation for the regressive form of the  $\Gamma$  curve for a powder with 36 perforations seemed natural at first glance.

Actually, however, an examination of the unburned powder rods obtained after firing has shown that no disintegration of the powder occurred at first. This was evidenced by the presence of many grains with strongly burned but otherwise intact perforations corresponding to  $\psi \approx 0.60$ , or by grains bearing signs of partial decomposition only (see right-hand photograph in fig. 31).

This condition indicates that the burning of powder with narrow perforations is more complex and depends on factors absent in the burning of powders of simple shapes and usually not taken into consideration.

It is therefore of importance to analyze the peculiarities involved in the burning of powders with narrow perforations and to develop a theoretical approach to the problem dealing with the deviation of such powders from the geometric law, as was disclosed in actual bomb tests.

## 1. THE EFFECT OF PROXIMATE CONTACT BETWEEN BURNING SURFACES

If two powder strips are burned separately in the open air, each strip will burn quietly. If, however, one strip is placed over the other while burning with the burning ends touching, burning at the points of contact will proceed more vigorously and gases will be forcefully ejected from the gap formed between the burning surfaces. This indicates that the gas pressure becomes increased.

An assumption has been made to the effect that if the surfaces of two grains were made to burn separately in one bomb and in close contact in another, the pressure between the contacting surfaces would be higher and the burning of the grains will proceed more vigorously.

### A. Tests with a Rod and a Tube.

This assumption was confirmed in an actual test.

Identical powder grains were burned simultaneously in small bombs ( $21.5 \text{ cm}^3$ ) wherein the grains were arranged differently.

The charge consisted of a tube and rod of nitroglycerin powder. The rod diameter was such that it could be inserted into the tube with a certain small clearance between them.

In one test the rod was placed in the bomb alongside the tube, and the other rod was inserted into the tube.

Due to its higher burning rate, nitroglycerin powder was found to give a sharper distinction between these parallel tests.

The results were as follows (fig. 66 - p, t and  $\Gamma$ , t curves): in

the first case the  $p, t$  curve was smooth, and in the second (rod inside tube) a sharp pressure increase was obtained at  $p \approx 100 \text{ kg/cm}^2$ ; following which the  $p, t$  curve became smooth again while remaining above the first one.

In the first case, curve  $\Gamma, \psi$  (fig. 67) shows a small amount of ballooning at  $\psi = 0.03$  and then slowly descends to  $\psi = 0.70$ , following which it drops rapidly because the web thickness of the tube is practically fully burned, and the final burning of the tube and the burning of the rod follow.

At the instant  $\psi = 0.90$  the tube is fully burned (thickness of tube was 1.75 mm and diameter of rod 5 mm) and the rod undergoes the last stages of burning.

In the case of the rod inserted into the tube, the  $\Gamma, \psi$  curve balloons sharply at  $\psi = 0.03$ , its apex corresponding to  $\psi = 0.04$ . The maximum ordinate at this point is almost twice as great as that of the corresponding ordinate of  $\Gamma$  of the first test; this is followed by an almost vertical drop down to the first curve ( $\psi = 0.06$ ), following which the curves are almost coincident.

In order to clarify these results, the test was repeated in open air. Upon igniting the rod simultaneously at both ends, it was ejected from the tube, apparently because of the pressure difference between the ends in the clearance present between the rod and tube.

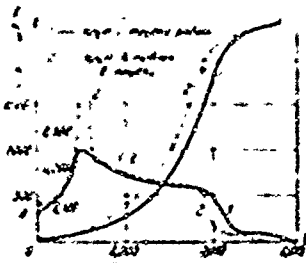


Fig. 66 - The Effect of Contacting Burning Surfaces on  $\Gamma$ , t.

1 - rod and tube side by side; 2 - rod inserted into tube.

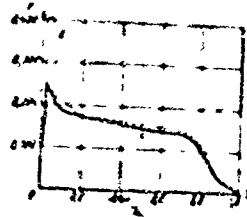


Fig. 67 - The Effect of Contacting Burning Surfaces on  $\Gamma$ ,  $\psi$ .

When tested in a bomb, the rate of gas formation rapidly increases because of the high burning rate of nitroglycerin powders, the close proximity of the burning surfaces and the small clearance, and ballooning occurs on the  $\Gamma$  curve. But due to the pressure difference which may occur at the opposite ends of the clearance, a string of relatively soft cordite would have been forced out of the tube. Thereafter, a close contact between the burning surfaces would have been obviated, and further burning would have continued under conditions almost analogous to the first test. This is indicated by the almost parallel path of the  $\Gamma$ ,  $\psi$  curves.

The fact that the burning in this case proceeds more vigorously than in the first test is indicated by the condition that the burning of the tube and rod in the second test was concluded ahead of the first one, as can be seen from the  $\Gamma$ , t curves in the diagram.

F-TS-7327-RE

223

GRAPHIC NOT REPRODUCIBLE

Actually, the drop of  $\Gamma$  corresponding to the end of the tube's burning occurs in the first case at  $t = 0.0095-0.0100$  sec, and in the second case - at  $t = 0.090$  sec. The full burning time in the first case is  $\tau = 0.0140$ , and  $0.0130$  sec in the second.

These tests are very valuable with regard to the theory of non-uniform powder burning, inasmuch as they show that the sharp increase in the rate of gas formation is not due to the increased surface area (which was the same in both tests), but, rather, to the increased rate of burning caused by the close contact of the burning surfaces and by higher pressure.

As soon as this contact is eliminated, the process proceeds normally. According to the geometric law of burning, all the powder surfaces must burn with the same rate, and a change in the mutual arrangement of the portions of the charge should not affect the law of gas formation.

#### B. Powders with Narrow Perforations

An identical phenomenon of accelerated gas formation should be observed in the case of powders with narrow and long perforations, wherein the burning surfaces are in close contact. The narrower the perforation, the closer is the contact between the perforation surfaces, and the more vigorous is the burning process. As the perforations are eroded, their surfaces spread apart and the intensity of burning decreases, and as a result the ordinates of the  $\Gamma, \psi$  curve become gradually reduced.



The fact that the burning rate before decomposition, determined by the formula

$$u_1 = \frac{e_1}{\int_0^1 p dt}$$

is considerably greater than the rate after decomposition, at which time the rate is normal, indicates that the burning rate is actually greater in perforated grains than in strip powders. Thus, the burning rate of Kisnensky's powder with narrow perforations before decomposition, corresponding to the point of inflexion on the pressure curve, is  $u_1 \approx 0.100$  mm/sec, compared with strip powder of the same composition whose normal rate is 0.075 mm/sec.

## 2. THE EFFECT OF THE LENGTH OF PERFORATION ON THE PROGRESSIVE BURNING OF POWDER

According to the geometric law of burning, the narrower and longer the perforation, the more progressive is the shape of the grain.

However, the narrower and longer the perforations, the greater will be the difference between the conditions of burning inside the perforations and at the outer surface, the more difficult will it be for the gases to leave the perforations, and the greater will be the pressure developed in them; and as a result the deviation from the geometric law towards regressive burning will be the greater.

In order to confirm these deductions, we are presenting below the results of tests in a manometric bomb for determining the progressive burning of powders with a large number of narrow

perforations of uniform cross section, but of varying length, and also the results of firing.

Tests for determining the effect of the length of perforations were made with powder No. 8: 36 perforations, relative length in a normal slab  $\frac{2c}{a_0} = 90$ .

The charge consisted of normal slabs, of slabs of the same cross-sectional area reduced to 1/4 length ( $\frac{2c}{a_0} = 22$ ), to 1/8 of the normal length ( $\frac{2c}{a_0} = 11$ ), and slabs reduced to 1/10 of normal length ( $\frac{2c}{a_0} = 9$ ). Perforation wall  $a_0 = 0.42$  mm.

If for the sake of simplicity we assume that the powder burns to the very end without decomposing, then, as the length of the slabs is decreased, the geometric progressivity  $\frac{S_K}{S_1}$  becomes smaller, and the exposed surface  $\frac{S_1}{\Lambda_1}$  becomes greater, as can be seen in Table 18.

Table 18

	$2c$	$\frac{2c}{4}$	$\frac{2c}{8}$	$\frac{2c}{10}$
$\frac{2c}{a_0}$	90	22	11	9
$\frac{S_1}{\Lambda_1}$	1.37	1.53	1.76	1.89
$\frac{S_K}{S_1}$	2.17	1.83	1.39	1.20

This data shows that a full-length slab ( $2c$ ) possesses a very high geometric progressivity (2.17), whereas a slab reduced 8 times in length has the progressivity of a grain with 7 perforations.

Theoretical curves of the variation of  $S/S_1$  corresponding to the geometric law of burning without decomposition are shown in the diagram of fig. 68a.

The geometric curves of progressivity ascend from the initial ordinate  $S/S_1 = 1$  in the form of a diverging cluster. The ordinates have a maximum value at the end of burning; as the length of the slabs is increased, the slope of the curve, and hence the progressivity, increases.

The test characteristics  $\Gamma = \frac{1}{p} \frac{d\psi}{dt}$  were calculated from these curves; then, in order to eliminate the influence of the varying exposure  $\frac{S_1}{\Lambda_1}$  entering into the values of  $\Gamma$ , the latter were subdivided into corresponding values of  $S_1/\Lambda_1$ , i.e., reduced not to the initial volume, but, rather, to the initial surface area  $S_1$ . We shall designate this value of  $\Gamma$ :  $\frac{S_1}{\Lambda_1} = \Gamma \frac{\Lambda_1}{S_1}$  by  $\Gamma_s$ ; the obtained curves of  $\Gamma_s$  as a function of  $\psi$  are shown in fig. 68.

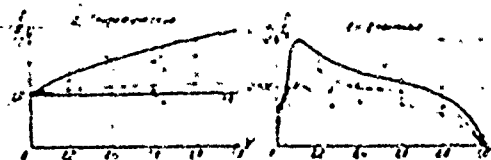


Fig. 68 - The Effect of the Length of Perforations on the Intensity of Gas Formation.

a) theoretical; b) test curves.

Were the geometric law applicable,  $\Gamma = \frac{S_1}{\Lambda_1} \frac{S}{S_1} u_1$ ;  $\Gamma_s = \frac{S}{S_1} u_1$ , i.e., the value of  $\Gamma_s$  at constant burning rate  $u_1$  would vary in proportion

GRAPHIC NOT REPRODUCIBLE

with  $S/S_1$ . Therefore the  $\Gamma_s, \psi$  curves should be of the same form and have the same relative arrangement as the curves of geometric progressivity  $\frac{S}{S_1}, \psi$  (fig. 68a).

An analysis of these tests shows the contrary to be true, as illustrated by the diagram in fig. 68b.

All the  $\Gamma_s$  curves have a sharp slope at first and a maximum at  $\psi \approx 0.10$ , following which their path is regressive. The highest curve is that for the slabs of the greatest length  $2c$ ; the shorter the slab, the lower is the  $\Gamma_s$  curve. The mutual disposition of the  $\Gamma_s$  curves is the same as of the  $S/S_1$  curves. But whereas the  $S/S_1$  curves proceed in the form of a diverging cluster and are the more progressive the greater the length of the slab, the experimental  $\Gamma_s$  curves show the reverse: they have a maximum divergence after a sharp ascent at  $\psi = 0.10$ , and then proceed in a converging cluster, whereby the greater the slab length, the more regressive is the curve.

For slabs  $\frac{2c}{8}$  in length the curve has even a small horizontal section.

Thus the longer the slab, the more will the burning of perforated powders deviate from the geometric law, the steeper will be the slope (ascent) of the  $\Gamma_s$  curve at the start of burning (while the perforations are still narrow), and the more regressive will the curve be thereafter. Decomposition commences at  $\psi \approx 0.70$  and the curves begin to drop to zero at  $\psi = 1$ .

The following conclusion can be derived from these tests: when powder is burned in a constant volume the change in the intensity of gas formation is the more regressive, the more progressive is the shape of the grain. The true or physical law of burning gives results which are opposite in character to those of the geometric law.

Further analysis will show that the  $r_s$  curve of the shortest slab 4 is more regressive than curve 3 representing a longer slab  $\left(\frac{2c}{8}\right)$ . Here the limited geometric progressivity begins to have its effect, and the conclusion is reached that for a powder grain of a given cross section there is such an optimum grain length at which the gas formation is most progressive (or least regressive)

$$\left(\frac{2c}{a_0} \approx 20-25\right) .$$

These bomb test results which are so paradoxical from the standpoint of the geometric law of burning were verified in actual firing tests (Table 19).

Table 19 - Results of Firing Using Powders of the Same Cross Section  
but of Different Lengths

Powder Specimen	$\frac{2e}{a_0}$	$\omega$ kg	$P_m$ kg/cm <sup>2</sup>	$v_A$ m/sec	$\frac{S_1}{A_1}$	$\frac{S_s}{S_1} = \phi_s$
Long ( $2c = 10A_0$ )	220	0.950	2285	613	1.39	1.89
Shortened ( $2c = 3A_0$ )	66	1.150	2290	655	1.44	1.81
Short ( $2c = A_0$ )	22	1.100	2285	648	1.59	1.54
Grade 9/7 (with 7 perforations)	24	1.200	2290	655	1.40	1.37

All the specimens gave the same value of  $p_m$ , though the longest specimen No. 1 having the most progressive shape produced this pressure with the smallest charge  $\omega = 0.950$ , which serves to explain why the velocity  $v_A$  was the lowest (613 m/sec).

The shortened specimen No. 2 having the least theoretically progressive shape permitted however, without elevating the pressure, to increase the charge to 1.150 kg and thus increase the muzzle velocity to 655 m/sec, i.e., it was actually found to be more progressive. Specimen No. 3, similarly to the bomb test, gave somewhat poorer results than specimen No. 2, producing the same pressure at a somewhat smaller charge (1.100 kg), and  $v_A$  was reduced to 648 m/sec.

These firing tests had shown that powders with narrow perforations give identical results in a bomb and when fired from a gun, and that powders with excessively long and narrow perforations are not profitable, notwithstanding their geometric progressivity. There is

a certain optimum length at which burning is most progressive; in guns at large values of  $\Delta$  this length may differ from that in a bomb at small values of  $\Delta$ .

Similarly, firing tests with tubular powders have confirmed the fact that longer tubes in an identical charge produce a higher pressure  $p_m$  and velocity  $v_\Delta$  compared with shortened tubes.

These tubes show that powders with narrow perforations do not follow the geometric law and that their deviation from the latter is the greater, the longer the perforation.

A comparison of the results obtained in firing shortened Kisnensky powders with 36 perforations (No. 2) and ordinary 9/7 powder (No. 4) indicate that notwithstanding the great difference between their geometric progressivity, the 9/7 powder produced the same results (at a considerably simpler manufacturing procedure).

### 3. THE FUNDAMENTAL THEORY OF NONUNIFORM BURNING OF PERFORATED POWDERS

As was mentioned above, a certain contradiction was disclosed between the actual and geometric law of burning even in powder grains of simple shapes.

Such contradictions were particularly sharply defined in the case of powders with narrow and long perforations. Test curves of the progressivity of burning are entirely contradictory to the theoretical curves; these deviations increase with the length of the perforations. What is the explanation thereof?

The basic concept of the geometric law rests on the condition that the pressure is always uniform at all the elements of the burning surface of the charge, and that hence the burning rate  $u = u_p$  is also uniform.

This condition would have been valid if the process of burning were to proceed very slowly to permit immediate equalization or balancing of the slightest pressure differences occurring at various points of the bomb, i.e., if the phenomenon were to proceed similarly to static processes.

Actually, of course, the burning process proceeds extremely rapidly to permit equalization of the pressure at different points of the charge, so that the burning rate is actually different at the various points of the burning surface. The difference in intensity must also be pronounced most sharply in the burning of powders with narrow perforations.

It can be easily proved that the rate of burning inside the perforations can be the same as the rate at the surface of the grain. In a chemically homogeneous powder composition the burning rates can be equal only at equal pressures. But if the pressure  $p''$  within the perforation equaled the outside pressure  $p'$ , the gases formed inside the perforations could not escape, unless a pressure difference were present. Therefore, if the inside and outside pressures were equal, the bomb would become filled with the gases formed at the outside surface of the powder only, while the gases in the



perforations would remain where formed, which condition is entirely improbable. Thus a simple reasoning shows that the burning rate inside and outside the grain cannot be the same.

By separately applying the pyrostatics formulas to the surface of the perforation and the outside grain surface, it can be shown quantitatively that the pressure inside a narrow perforation cannot equal the pressure at the outside grain surface, and that the pressure increase inside the perforation must proceed considerably more rapidly.

We shall make a preliminary analysis of the values governing the pressure increase obtained in burning powders of simple shapes without perforations, assuming that the grains are uniformly distributed in the bomb, or that only one grain is being burned.

We have introduced the following expression for determining the pressure increase in a constant volume:

$$\frac{dp}{dt} = \frac{f\Delta \left(1 - \frac{\Delta}{\delta}\right)}{\Lambda_{\psi}^2} \frac{S_1}{\Lambda_1} \frac{S}{S_1} u_1 p.$$

For the initial stage of the burning process  $S \approx S_1$

$$\Lambda_{\psi} = 1 - \frac{\Delta}{\delta} - \Delta \left( \alpha - \frac{1}{\delta} \right) \psi \approx 1 - \frac{\Delta}{\delta};$$

then

$$\frac{dp}{dt} = \frac{f\Delta}{1 - \frac{\Delta}{\delta}} \frac{S_1}{\Lambda_1} u_1 p = \frac{f\omega}{W_0 - \frac{\omega}{\delta}} \frac{S_1}{\Lambda_1} u_1 p,$$

but  $\frac{\omega}{\Delta_1} = \delta$  - powder density, and

$$\frac{dp}{dt} = f\delta u_1 \frac{S_1}{W_0 - \frac{\omega}{\delta}} p. \quad (50)$$

Designating  $W_0 - \frac{\omega}{\delta} = V$ , we get

$$\frac{dp}{dt} = f\delta u_1 \frac{S_1}{V} p$$

and hence for a given type of powder ( $f, \delta, u_1$ ) and pressure  $p$ , the pressure increase  $dp/dt$  is determined by the ratio between the burning surface area of the powder and the volume in which the gas is separated from the powder surface.

We shall designate this ratio by  $\zeta$ :

$$\zeta = S/V.$$

Burning inside the powder perforation can be viewed as consisting of two consecutive processes:

- 1) accumulation of gases separated from the surface of the perforation inside the perforation space;
- 2) outflow of the accumulated gases from the perforation if the inside pressure exceeds the pressure at the surface of the grain.

We shall apply formula (50) separately to burning at the inside surface of the perforations and to burning at the outside grain surface and compare the results.

Let us designate the initial volume of each perforation  $W_K$  and its surface area  $S_K$ ; the total number of grains in the charge is  $N$ , and the number of perforations in each grain is  $n$ .

If we assume that the igniter pressure  $p_B$  is the same at the outer surface and inside each perforation, then:

$$\text{in the perforation } \frac{dp''}{dt} = f\delta u_1 p_B \zeta'',$$

where

$$\zeta'' = \frac{S_K}{W_K} = \frac{\pi d \cdot 2c}{\frac{\pi d^2 2c}{4}} = \frac{4}{d};$$

and at the outer grain surface  $S'$

$$\frac{dp'}{dt} = f\delta u_1 p_B \zeta',$$

where  $\zeta'$  is the ratio of the entire surface area  $S'$  to the volume within which the gases are separated from this surface, i.e.,

$$\zeta' = \frac{S'}{W_0 - \frac{\omega}{\delta} - NnW_K}.$$

Bearing in mind that  $\frac{\omega}{\delta} = \Lambda_1$ , where  $\Lambda_1$  is the volume of the entire charge, and dividing the numerator and denominator  $\zeta'$  by

$\frac{\omega}{\delta} = \Lambda_1$ , we get:

$$\xi' = \frac{1}{\Lambda_1 \frac{\pi_0}{\Lambda_1} - 1 - \frac{Nn\pi_K}{\Lambda_1}} = \frac{S_1}{\Lambda_1} \frac{S'}{S_1} \frac{1}{\frac{\sigma}{\Delta} - 1 - \frac{Nn\pi_K}{\Lambda_1}}.$$

Calculations show that for a standard grain with 7 perforations at  $\Delta = 0.20 \xi'' \approx 70 \xi'$ ; therefore the ratio between the rate of pressure increase in the perforation and the rate at the outer surface will be considerably greater (of the order of several tens):

$$\frac{dp''}{dt} \gg \frac{dp'}{dt} \quad \text{and} \quad p'' > p'.$$

Therefore, even if the pressure in a narrow perforation and at the outside surface are equal at a certain moment, the pressure inside the perforation will immediately begin to increase at a faster rate than at the outside surface, and hence the burning rate  $u'' = u_1 p''$  will be higher.

All the reasonings presented above relate to the start of burning and would be entirely valid if no gases were to flow out of the perforations. Actually, inasmuch as the pressure will increase more rapidly inside the perforations, the gas will escape because of the resulting pressure difference, so that the free space within the perforation will be increased and the outside free space, wherein are also collected the gases separating from the outside surface, will be decreased. As a result, the pressure difference will become reduced when both the perforation and the outside surface are burning, and will gradually become equalized.

However, due to the extremely high speed of this phenomenon, the gases formed in the perforations are incapable of fully escaping from the narrow openings and become accumulated in the perforations, the pressure increases as a result and in turn increases the rate of burning, so that burning in the perforations at a given pressure within a bomb must invariably proceed at a higher rate than at the outside surfaces of the grain.

Thus the presence of narrow and long perforations in the powder will always cause nonuniform burning in the perforations and at the grain surface, and this nonuniformity results in the anomalous curves of progressivity  $\Gamma, \psi$  presented above (see diagrams in figs. 48, 49, 52 and 53).

If the loading density  $\Delta$  is increased, the corresponding value of  $\zeta''$  for each perforation remains unchanged, the value of  $\zeta'$  for the outside surface increases (because the entire  $\zeta'$  fraction increases with the increase of  $\Delta$ ), and the ratio  $\frac{\zeta''}{\zeta'}$  decreases and tends toward unity.

Tests have shown that the  $\Gamma, \psi$  curves at small values of  $\Delta$  actually become more regressive.

# GRAPHIC NOT REPRODUCIBLE

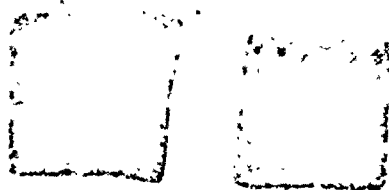


Fig. 69 - Burning of Kisnemy's Powder with Very Narrow Perforations.

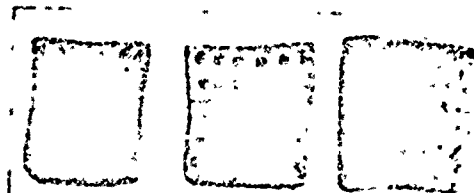


Fig. 70 - Burning of Kisnemy's Powder with Very Narrow Perforations.

The presence of a considerably increased pressure in very narrow and long perforations can be seen in photographs of slabs of Kisnemy's powders No. 9 and 10 (figs. 69 and 70) ejected from a gun before they were fully burned. The photographs on the left show slabs of Kisnemy's powders before burning, the perforations are so narrow (0.1-0.2 mm) that they can be hardly seen because of their fused openings; the photographs on the right are of grains

ejected from a gun. Many of the perforations are eroded, which condition can be due only to the presence of a high pressure within the perforations; similar erosions were observed also on the side surfaces of the slabs. The perforations are almost circular in shape.

#### 4. EFFECT PRODUCED BY NONUNIFORM BURNING OF PERFORATED POWDERS ON THE SHAPE OF THE $\Gamma$ CURVE

We shall now show that nonuniform burning and excessive gas pressure in narrow perforations can serve to explain the steep ascent at the start and the continuous drop of the  $\Gamma, \psi$  curve obtained from the analysis of experimental  $p, t$  curves obtained with powders having narrow perforations.

We have the following designations:

$S'$  - outside surface area of burning grain;

$S''$  - combined surface area of all the perforations in the grain;

$S = S' + S''$  - total surface area of the grain;

$\Lambda_1$  - initial volume of grain;

$u'$  - burning rate at the outside grain surface ( $u' = u_1 p'$ );

$u''$  - burning rate inside the perforations ( $u'' = u_1 p''$ ).

In order to simplify the analysis of the phenomenon, let us assume that the burning rate inside the perforations is uniform and that the burning rate along the entire outside surface is likewise constant.

Let us see now how the test curve of progressivity  $\Gamma = \frac{1}{p} \cdot \frac{d\psi}{dt}$  in the case of the geometric law will differ from the same curve based on actual burning proceeding with different rates at the outside surface and in the perforations.

Let us assume that at a given instant the same portion of the charge  $\Psi$  was burned in both cases, and that the pressure at the outside surface equaled  $p'$  and on the inside surface -  $p''$ ; it may be assumed that the crusher used in the bomb test records a pressure  $p'$ .

Then, in the first case (geometric law of burning), the burning rate on all the surfaces will be the same:

$$u'' = u'; p'' = p'.$$

Using the general formula for the rate of gas formation as the basis, we can write:

$$\left(\frac{d\psi}{dt}\right)_I = \frac{S}{\Lambda_1} u = \frac{S' + S''}{\Lambda_1} u' = \frac{S' + S''}{\Lambda_1} u_1 p';$$

$$\Gamma_I = \frac{1}{p'} \left(\frac{d\psi}{dt}\right)_I = \frac{S' + S''}{\Lambda_1} u_1.$$

In the second case (actual burning), the burning rate differs:

$$u'' > u'; p'' > p'.$$

The surface area of the perforations  $S''$  burns with the rate  $u''$ , and the outside surface  $S'$  - with the rate  $u'$ .

We get:

$$\left(\frac{d\psi}{dt}\right)_{II} = \frac{S'u' + S''u''}{\Lambda_1} = \frac{\left(S' + S'' \frac{u''}{u'}\right)}{\Lambda_1} u' = \frac{\left(S' + S'' \frac{p''}{p'}\right)}{\Lambda_1} u_1 p';$$

$$\Gamma_{II} = \frac{1}{p'} \left(\frac{d\psi}{dt}\right)_{II} = \frac{\left(S' + S'' \frac{p''}{p'}\right)}{\Lambda_1} u_1.$$



A comparison of the  $\Gamma_I$  and  $\Gamma_{II}$  expressions will show that they differ by their  $p''/p'$  factors alongside the surface  $S''$  appearing in parenthesis.

Inasmuch as  $\frac{p''}{p'} > 1$ ,  $\Gamma_{II} > \Gamma_I$ , as observed in comparing the theoretical and test curves of  $\Gamma$ .

Hence, when burning is not uniform, the behavior of the powder is such as if the surface area of its perforations were increasing with respect to  $p''/p'$ .

Actually this represents an increased rate of gas formation due to the increased burning rate in the perforations.

We thus arrive at the following conclusion: if the burning of the powder is not uniform, the pressure and burning rate in the perforations being higher than at the outside surface, then at a given  $\psi$  the intensity of gas formation  $\Gamma_{II}$  must always be greater than  $\Gamma_I$ , when calculated with the assumption that the burning of the powder is uniform.

The difference between the rates of gas formation based on actual and geometric laws of burning will depend upon the ratio

$$\frac{u''}{u'} = \frac{u_1 p''}{u_1 p'} = \frac{p''}{p'}$$

As burning progresses, the diameter of the perforation increases, and the ratio  $\frac{4}{d}$  and hence of  $\frac{\zeta''}{\zeta'}$  becomes smaller; the  $\frac{p''}{p'}$  ratio will decrease also and the  $\Gamma_{II}$  and  $\Gamma_I$  curves will converge. This is the very condition actually observed on the  $\Gamma, \psi$  curves.

Thus under conditions of actual burning of progressive powder with narrow perforations in a constant volume the intensity of gas formation will be considerably greater at the start of burning, and the  $\Gamma, \psi$  curve will be situated considerably higher than the theoretical curve.

This difference becomes smaller as burning progresses, and the intensity of gas formation will differ from the theoretical to a smaller degree. During the entire process of burning of progressive powder the value of  $\Gamma$  may generally decrease and hence the burning will be regressive.

The narrower the perforations and the greater their number, the higher will be the ratio between the perforation surface area  $S''$  and the total surface area  $S_1$ , the sharper will be the influence of nonuniform burning and the greater will be the deviation from the geometric law, so that progressive powder grains will actually burn regressively, which is the case observed in the burning of Kisnemy's powders with 36 perforations.

#### 5. BURNING OF POWDER WITH NARROW PERFORATIONS IN A GUN

Tests show that the  $\Gamma, \psi$  curves at small values of  $\Delta$  are more regressive than at high values of  $\Delta$ .

This behavior is most important in clarifying the actual burning of perforated powders in a gun, where the initial loading density is very high (of the order of 0.50-0.70), and decreases continuously as the shell moves through the bore.

It was shown in the theory of nonuniform burning of powder

that as the loading density decreases, the difference increases between the values  $\zeta'$  and  $\zeta''$  characterizing the rate of gas pressure increase at the outer surface and inside the powder perforations.

For powders with 7 perforations at  $\Delta = 0.20$   $\zeta'' \approx 70\zeta'$ , the  $\Gamma, \Psi$  curve of the intensity of gas formation is also regressive.

The powder commences to burn in a gun at considerably higher loading densities ( $\Delta_0 = 0.60-0.70$ ), at  $\Delta_0 = 0.70$   $\zeta'' \approx 8\zeta'$  for the same type of powder with 7 perforations, i.e., the difference becomes equalized. Burning at this constant value of  $\Delta_0 = 0.70$  would have occurred under more uniform conditions.

In addition, due to the movement of the shell through the bore, the space behind it increases continuously, and the loading density in this variable volume continues to decrease during the entire burning process ( $\Delta = \frac{\omega}{V_0 + s\ell}$ ). This results in a continuous variation of the  $\zeta'' : \zeta'$  ratio, whereby this ratio increases when  $\Delta$  is reduced, which serves to increase the intensity of gas formation  $\Gamma$  and increases the progressive burning as the shell moves through the bore.

Thus in attempting to reach a conclusion regarding the burning of powder in a gun, we cannot consider its burning in a bomb at one constant loading density as being representative and assume that the obtained  $\Gamma, \Psi$  curve characterizes the intensity of gas formation in a gun. Such a conclusion would be incorrect. The burning of powder must be considered in its relation to the conditions of loading and burning taken as a whole.

Therefore, in order to calculate the intensity of gas formation when burning powder in a gun, it is first necessary to determine the  $\Gamma, \psi$  curves at constant but different values of  $\Delta$  by means of bomb tests, and to determine the effect of  $\Delta$  on the characteristic change of intensity of gas formation. Then, taking into account the initial loading density  $\Delta_0$  in a gun, it is necessary to extrapolate the experimental  $\Gamma, \psi$  curves obtained in a bomb at smaller values of  $\Delta$  for the given loading density  $\Delta_0$ . Thereafter, bearing in mind that the loading density in a gun decreases continuously from  $\Delta_0$  to  $\Delta_K = \frac{w}{w_0 + s l_K}$  (where  $l_K$  is the distance traversed by the shell at the end of burning of the powder), it is necessary to go over, as  $\psi$  increases, from the  $\Gamma, \psi$  curve at  $\Delta = \Delta_0$  to the  $\Gamma, \psi$  curves corresponding to successively smaller constant densities of loading.

As a result, the  $\Gamma, \psi$  curve of the intensity of gas formation for a variable loading density will differ from each  $\Gamma, \psi$  curve obtained at constant values of  $\Delta$ . As shown in fig. 71 by a solid curve, it can be even more progressive, the progressivity being the higher the greater the initial density of loading.

At low initial loading density  $\Delta_0$ , the change in the regressive characteristic of the  $\Gamma, \psi$  curves obtained at constant  $\Delta$  will be insignificant, and in such a case the burning may be regressive also at a variable value of  $\Delta$  (fig. 72).

The effect of the value of  $\Delta_0$  on progressive burning will serve as an explanation of the following very interesting fact observed in the firing of guns with Kisnensky's powders: in one gun a charge

consisting of Kisnemy's powder with 36 perforations at a high loading density gave better results than strip powder ( $p_{\max}$  was lower at the same value of  $v_A$ ), whereas another gun at a small value of  $\Delta_0$  loaded with the same powder gave poorer results (the same  $v_A$  velocity at a considerably higher pressure  $p_{\max}$ ).

This fact can be explained only by means of the theory of nonuniform burning.

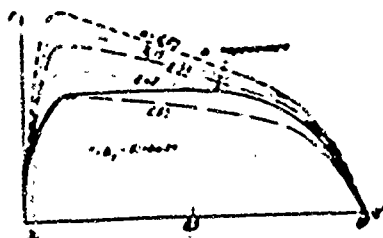


Fig. 71 - Intensity of Gas Formation in a Gun at a High Value of  $\Delta_0$ .

1)  $\Delta$  - variable; 2)  $\Delta_0$  - large.

The higher the loading density, the more uniform will be the conditions of burning inside the perforations and at the outside surface, and the more closely will actual burning approach the geometric law.

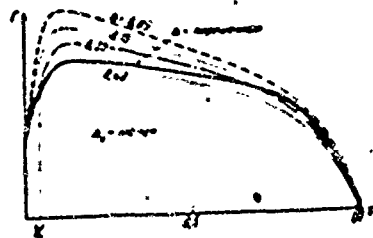


Fig. 72 - Intensity of Gas Formation in a Gun at a Small Value of  $\Delta_0$ .

Fig. 72 - (Cont'd.)

- 1)  $\Delta$  - variable; 2)  $\Delta_0$  - small.

Only by considering the process of burning in conjunction with all the factors influencing its characteristics, can we arrive at a correct conclusion, on the basis of the theory of nonuniform burning, regarding the true burning of a powder charge in the bore of a gun when the latter is fired. The theory of nonuniform burning had disclosed the fundamental laws governing the burning of powders with narrow perforations and had made it possible to explain the reasons for the unsatisfactory progressive burning of Kisnensky's powders.

#### CHAPTER 4 - THE USE OF INTEGRAL CURVES

##### 1. THE PRESSURE IMPULSE OF POWDER GASES AS THE BURNING CHARACTERISTIC OF POWDER

Using the pressure curve obtained from a bomb test, the corresponding values of  $\psi$  can be found from the values of the successively increasing values of  $p$ ; the test characteristic of progressivity - the function  $\Gamma = \frac{1}{p} \frac{d\psi}{dt}$  with relation to  $t$  and  $\psi$  can then be calculated, as well as the successively increasing values of  $\int_0^t p dt$ .

The obtained data is used for constructing  $\Gamma$ ,  $\psi$  and  $\int_0^t p dt$ ,  $\psi$  graphs. We shall introduce the designation  $I = \int_0^t p dt$ .

The value of the  $\Gamma$  function as an analytic function of the powder burning process was discussed in detail earlier: its form depends on the dimensions and shape of the powder, on the characteristics and burning conditions of the powder, and takes into consideration the ignition characteristics and the heterogeneity of the powder composition - both chemical (flegmatization) and physical (porosity).

The integral curve  $I, \psi$  is likewise a characteristic of the burning of powder, whose form changes depending upon the above-mentioned factors.

Actually, the tangent of the angle formed by a line tangent to curve  $I, \psi$  is the inverse of  $\Gamma$  (fig. 73):

$$\tan \beta = \frac{dI}{d\psi} = \frac{p dt}{d\psi} = \frac{1}{\Gamma}$$

or

$$\Gamma = \cotan \beta.$$

Inasmuch as the value of  $\Gamma$  increases when the burning of the powder is progressive, angle  $\beta$  will become smaller and the concave side of the  $\int_0^t p dt, \psi$  curve will be directed towards the  $\psi$ -axis; when burning is regressive, the convex side of the  $I, \psi$  curve will be directed towards the  $\psi$ -axis. Therefore, the  $I, \psi$  curve obtained from the bomb test pressure curve can also serve as a characteristic of progressivity under actual conditions of burning.

We are presenting below schematic diagrams of  $\Gamma, \psi$  and  $I, \psi$  curves obtained with a weak and strong igniter (figs. 74 and 75). The slower the full ignition, the longer will be the portion of the curve corresponding to gradual pressure increase, and the more rapidly will the area under the  $I$  curve increase at small variations of  $\psi$ . The inflexion of the  $I, \psi$  curve at point  $a$  corresponds to the apex of "ballooning" on the  $\Gamma, \psi$  curve (point  $a'$ ).

The nature of ignition considerably affects the form of the initial portions of the  $I, \psi$  curve (up to  $\psi = 0.15-0.20$ ).

Therefore, in order to obtain results corresponding to actual firing conditions, the igniter pressure  $p_B$  for use in bomb tests must be the same as that used in firing of a gun with the same powder.

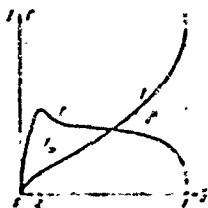


Fig. 73 - Relation Between  $I, \psi$  and  $\Gamma, \psi$  Curves.

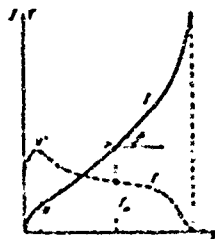


Fig. 74 -  $I, \psi$  and  $\Gamma, \psi$  Curves Obtained with a Weak Igniter.

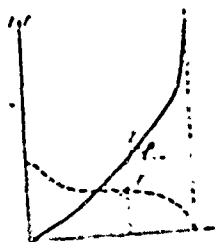


Fig. 75 -  $I, \psi$  and  $\Gamma, \psi$  Curves Obtained with a Strong Igniter.



Fig. 76 - Relative Pressure Impulse  $I/I_K$  as a Function of  $\psi$ .

It is known from pyrostatics that  $I_K = \frac{e_1}{u_1}$  and  $I = \frac{e}{u_1} = \frac{e_1}{u_1} \frac{e}{e_1} = I_K z$ ; hence  $I$  is proportional to  $z$ , and the  $I, \psi$  curve is analogous to the  $z, \psi$  curve. The  $z, \psi$  curves were presented in the section of general pyrostatics; hence the theoretical  $I, \psi$  or  $\frac{e_1}{u_1} z$  curves will have the form (when the coordinate axes change places) shown in fig. 76.



Curve 1 in this figure corresponds to the change of pressure impulse of tubular powder, 2 - of strip powder, 3 - of a cube at the same value of  $I_K = \frac{e_1}{u_1}$ .

The thicker the powder at a given burning rate  $u_1$ , the higher will be the integral curve  $I, \psi$  on the diagram; the higher the burning rate at a given thickness, the lower will be the location of the  $I, \psi$  curve.

## 2. THE USE OF $\int_0^t p dt$ FOR DETERMINING THE BURNING RATE $u_1$ .

The burning rate at  $p = 1$ , i.e.,  $u_1$ , is determined by formula

$$u_1 = \frac{e_1}{\int_0^{t_K} p dt} = \frac{e_1}{\int_0^{\psi=1} p dt},$$

where  $e_1$  is one half the thickness of the burning web,  $\int_0^1 p dt = I_K$  is the complete integral determined from bomb tests.



Fig. 77 - The Application of  $\int p dt$  for Determining  $u_1$  for Regressive Powders.

This formula would apply if ignition were instantaneous and the thickness of the powder were uniform throughout and equal to an

average value. Actually of course the powder thickness in a charge is not uniform. In addition to elements of an average thickness, there are present also thinner and thicker elements, and the complete integral  $\int_0^1 p dt$  determined in bomb tests corresponds to the burning of an element of maximum thickness, which thickness is usually unknown. Actual powder measurements permit determining only the approximate average thickness of the webs of the grains composing the charge. Hence, in order to determine  $u_1$ , the value of  $\int p dt$  used in the denominator must correspond to the mean powder thickness  $e_1$  cp ( $e_1$  average).

In order to determine  $\int p dt = I_1$  corresponding to the average thickness  $e_1$  cp, a diagram must be constructed of the variation of  $I$  as a function of  $\psi$ . For strip and tubular powders the  $\int p dt, \psi$  curve usually undergoes a sharp deflection upwards after  $\psi \approx 0.90$ ; this corresponds to the end burning process of the thicker elements. Hence, in order to determine  $I_1$  cp corresponding to the burning of the mean thickness, the second half of the  $I, \psi$  curve must be extended or prolonged using an accurate French curve, when  $\psi$  changes within the limits of 0.5-0.9, until this extension along the basic direction of the curve intercepts the ordinate at  $\psi = 1$  (fig. 77).

The ordinate thus obtained will be smaller than the full integral  $\int_0^1 p dt = I_K$ , and will correspond to the average thickness  $e_1$  cp.  
Then

$$u_1 = \frac{e_1 \text{ cp}}{I_1 \text{ cp}}.$$

Inasmuch as in the case of weak igniters a considerable variation will be obtained in the individual curves during the ignition process

(up to  $\psi \approx 0.10$ ), then, in order to obtain a more reliable result as regards the basic region of burning conforming to the law, the following method is suggested for determining  $u_1$ .

Using the geometric law as the basis, with the shape of the powder and dimensions ratio known, the  $\chi, \lambda$  characteristics are computed for short tubes, strips or plates, or  $\chi, \lambda, \mu$  for a slab or cube. Using formula

$$\psi = \chi z + \lambda \chi z^2 -$$

and assuming that  $\psi = 0.10$  and  $0.90$ , the corresponding values  $z_{0.10}$  and  $z_{0.90}$  are computed, and the thicknesses  $e_{0.10} = e_1 z_{0.10}$  and  $e_{0.90} = e_1 z_{0.90}$  and the burning rate in this region are determined by means of formula

$$u_1 = \frac{e_{0.90} - e_{0.10}}{\int_{0.10}^{0.90} p dt},$$

where  $\int_{0.10}^{0.90} p dt$  is obtained directly from the  $I, \psi$  diagram (fig. 78).



Fig. 78 - Determining  $u_1$  at Weak Igniter Pressure.

F-TS-7327-RE

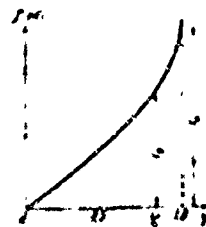


Fig. 79 - Determining  $u_1$  for Powders of Progressive Shapes.

251

GRAPHIC NOT REPRODUCIBLE

In the case of progressive powder grains, if the grain dimensions are known, it is necessary to calculate  $\psi_s$  at the instant of decomposition (using the assumption that the burning of the grain is progressive), obtain from the  $\int p dt$ ,  $\psi$  diagram the value of  $I_s = \int_0^{\psi_s} p dt$  (fig. 79), and, assuming that the mean web thickness already burned at the time is  $e_1$  cp, determine the value of  $u_1$  by formula:

$$u_1 = \frac{e_1 \text{ cp}}{\int_0^{\psi_s} p dt} = \frac{e_1 \text{ cp}}{I_s}.$$

Inasmuch as in actual practice burning inside the perforations and at the outside surface (in powders with narrow perforations) proceeds at different rates, the determination of rate  $u_1$  is conditional and depends on  $\Delta$ , and can give only comparative results for a given loading density.

### 3. INTEGRAL CURVES AS CRITERIA FOR THE VERIFICATION OF THE BURNING RATE LAW

Using the burning rate law  $u = u_1 p$  as a basis, it was shown above that the full pressure impulse  $\int_0^{t_K} p dt = \frac{e_1}{u_1}$  does not depend on the loading density.

It can be easily shown that in the case of different burning rate laws  $u = ap + b$  or  $u = Ap^\nu$ , where  $\nu < 1$ , the magnitude of  $\int_0^{t_K} p dt$  must increase with the increase of the loading density.

Indeed, if  $u = \frac{de}{dt} = ap + b$ , then

$$de = apdt + bdt;$$

$$e_1 = \int_0^{t_K} p dt + bt_K;$$

$$\int_0^{t_K} p dt = \frac{e_1}{a} - \frac{b}{a} t_K;$$

but the full time of burning  $t_K$  decreases with increase of  $\Delta$  (it depends on  $\Delta$ ). Hence, if the law is  $u = ap + b$ ,  $\int_0^{t_K} p dt$  will be the greater, the higher the loading density, i.e., it depends on  $\Delta$ .

The same can be said for the law  $u = Ap^\nu$ :

$$u = \frac{de}{dt} = Ap^\nu;$$

$$de = Ap^\nu dt \frac{p^{1-\nu}}{p^{1-\nu}} = \frac{A}{p^{1-\nu}} p dt.$$

When integrating, the average value of  $p^{1-\nu}$  is taken out of the integral:

$$e = \frac{A}{(p^{1-\nu})_{cp}} \int_0^t p dt \text{ and } e_1 = \frac{A}{(p^{1-\nu})_{cpK}} \int_0^{t_K} p dt,$$

whence

$$\int_0^{t_K} p dt = \frac{e_1}{A} (p^{1-\nu})_{cp_K}. \quad (\text{The subscript } cp \text{ stands for "average."})$$

But as the loading density is increased,  $(p^{1-\nu})_{cp_K}$  increases also, because the maximum and mean pressure become greater. Hence, for the law  $u = Ap^\nu$ , where  $\nu < 1$ ,  $\int_0^{t_K} p dt$  will be the greater, the higher the density of loading.

Thus the dependence or independence of the  $\int_0^{t_K} p dt$  integral on the loading density constitutes the basic criterion in the validity of the given burning rate law.

If the full pressure impulse during the burning of powder does not depend on the loading density, this condition can prevail only in the case of the burning rate law  $u = u_1 p$ .

If, however, the impulse becomes greater as the loading density increases, this condition can apply only to the burning rate law  $u = Ap^\nu$ , where  $\nu < 1$  or  $u = ap + b$ .

The above criterion can also be formulated as follows:

If upon increasing the loading density the integral curves  $\int p dt$  as a function of  $\psi$  coincide with each other, the burning rate law  $u = u_1 p$  (where  $p$  is of the first degree or  $\nu = 1$ ) is valid.

If upon increasing the loading density the integral curves  $\int p dt$  as a function of  $\psi$  proceed from the origin of the coordinates as a diverging cluster, the higher - the greater the value of  $\Delta$ , then the law  $u = Ap^\nu$ , where  $\nu < 1$ , or the law  $u = ap + b$  is valid.

#### 4. THE USE OF INTEGRAL CURVES FOR VERIFYING THE BURNING RATE LAW

##### A. The Application of Diagrams to Powders of Simple Shapes.

In order to establish the burning rate law, we had conducted tests in 1924-25 with powders of simple shapes (strip, short tubes) in order to obtain the phenomenon in a purer form and eliminate the effect of narrow and long perforations [4].

We had chosen for our first tests strip powder "CP" ( $2e_1 \approx 1$  mm), which has an exceptionally regular shape and is most uniform in thickness and in cross section. Plates were selected of the most uniform thicknesses and were tested in a bomb at a loading density of  $\Delta = 0.159, 0.209$  and  $0.259$  using a strong igniter  $p_B \approx 120$  kg/cm<sup>2</sup>.

These plates were burned in simultaneous tests at a constant loading density of  $\Delta = 0.209$  in order to obtain a picture of the scattering of the integral curves under identical test conditions. The results of both test series are presented in the diagrams of fig. 80a and b.

The  $I, \psi$  curves at different values of  $\Delta$  lie just as closely to one another as do the curves at the same value of  $\Delta$ ; the difference between the values of  $\int p dt$  at different  $\Delta$  lies within the allowable test limits. No divergence of the integral curves (cluster) is observed.

Therefore, it may be considered proved that for strip powder of properly chosen thickness the value of  $\int p dt$  for the given value of  $\psi$  does not depend on the loading density  $\Delta$ , this condition being true only for the burning rate law  $u = u_1 p$ . Hence it may be considered

proved that for pyroxylin strip powder the burning rate is proportional to pressure to the first power.

Thereafter, the following was established on the basis of many tests with powders of the most diversified compositions and with webs of different thicknesses.

1) Powders in the form of simple regressive shapes - strip, rod, short tube with a relatively wide perforation - burn in such a manner that at  $\Delta$  varying from 0.12 to 0.25,  $\int_0^{\psi} p dt$  does not depend on the loading density and the integral I,  $\psi$  curves proceed in the form of a coinciding cluster (figs. 81 and 82).

This coincidence is most complete for powders of uniform thickness and when using a strong igniter ( $p_B = 100-150 \text{ kg/cm}^2$ ), which insures almost instantaneous ignition in a bomb.

Tubular powders containing a solid solvent (trotyl + pyroxylin) produce  $\Gamma, \psi$  curves which are free of "ballooning" and integral I,  $\psi$  curves in the form of straight lines from  $\psi = 0$  to  $\psi \approx 0.90-0.95$  (see fig. 81).

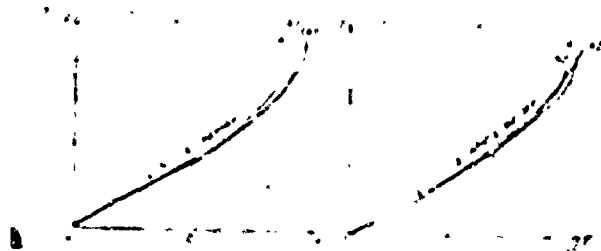


Fig. 80 - Integral Curves.

a) at different values of  $\Delta$ ; b) at the same value of  $\Delta$ ; 1) different values of  $\Delta$ ; 2) same value of  $\Delta$ .



Tubular powders with volatile solvents (pyroxylin and poorly volatile nitroglycerin) always produce "ballooning" on the  $\Gamma, \psi$  curves, which gradually disappears in the first third of the burning process. However, the mutual disposition of the integral  $I, \psi$  curves does not change - they proceed in the form of a coinciding cluster and have a certain amount of curvature in the first third of the process (fig. 82).

Thus, also these tests with pyroxylin powders and powders with a solid solvent in the form of short tubes had shown that when they are burned in a bomb at loading densities of 0.15-0.25, the burning rate law  $u = u_1 p$  is valid.

Similar data was obtained with large plates prepared by cutting up powder blocks with a solid solvent employed in certain types of rocket shells.

2) The same powders of simple shapes without narrow perforations burn at low loading densities ( $\Delta \approx 0.10$ ) in a manner where the full pressure impulse  $\int_0^{t_K} p dt = I_K$  decreases with the decrease of  $\Delta$ ; this behavior in the case of the  $u = u_1 p$  law corresponds to the increase of the burning rate  $u_1$  as  $\Delta$  decreases.

Figures 83a and 83b show the nature of the variation of  $\int_{\psi=0.05}^{\psi=0.75} p dt$  for "CΠ" powder ( $2e_1 = 1$  mm) and the corresponding variation of the value of  $u_1$  from 0.120 mm/sec : kg/cm<sup>2</sup> at  $\Delta = 0.02$  to 0.077 mm/sec : kg/cm<sup>2</sup> at  $\Delta = 0.12$ . At  $\Delta > 0.12$   $I_K$  and  $u_1$  retain their values.

The same condition, but with a more drastic change of  $I_K$  when  $\Delta$  is decreased, is observed in A.I. Kokhanov's tests with powders 2.4 mm thick.  $I_K = \text{const}$  within  $\Delta = 0.12-0.22$ , at  $\Delta = 0.02$  the value of  $I_K$  decreases almost 4-fold (fig. 84).

## GRAPHIC NOT REPRODUCIBLE

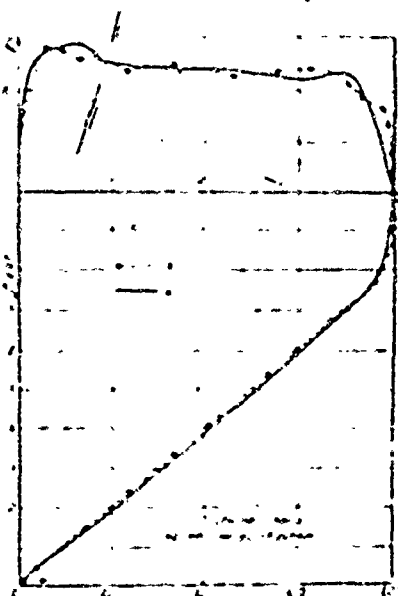


Fig. 81 -  $\int p dt, \psi$  and  $\Gamma, \psi$  Curves for Tubular Powder with Solid Solvent.

a) Tubular powder with solid solvent.

Such a decrease of  $\int p dt$  at low loading densities is observed only with powder thicknesses exceeding 0.7-1.0 mm.

3) In the case of thin pyroxylin powders in the form of small plates (hunting rifle powders "GLUKHAR," "VOLK" and others), the value of  $I_K$  remains practically unchanged when the loading density is varied from 0.157 to 0.02.

Therefore, in the case of pyroxylin powders of simple shapes, the variation of the  $\int_0^{t_K} p dt$  integral with change of  $\Delta$ , or its constancy, depends not on the nature of the powder mass, but, rather, on the burning characteristic of the powder.

Thick powders at high values of  $\Delta$  and thin ones at both high and low values of  $\Delta$  give a constant  $\int_0^{t_K} p dt$ . In the case of thick powders at small values of  $\Delta$  ( $< 0.10$ ),  $\int_0^{t_K} p dt$  decreases with decrease of  $\Delta$ , which corresponds to an increase of the burning rate  $u_1$  when the  $u = u_1 p$  law applies.

## GRAPHIC NOT REPRODUCIBLE

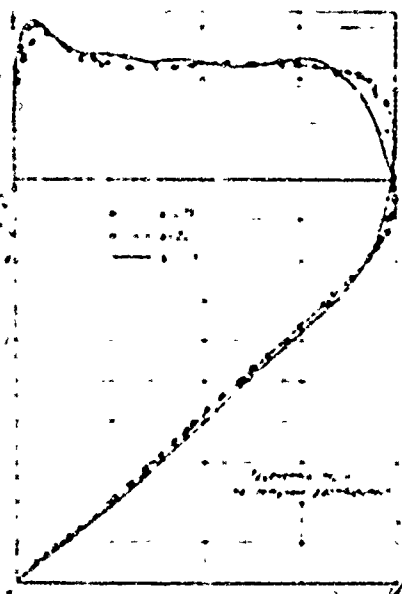


Fig. 82 -  $\int p dt, \psi$  and  $\Gamma, \psi$  Curves for Tubular Powder with Volatile Solvent.

1) Tubular powder with volatile solvent.

How can the above results be explained?

It is most reasonable and most simple to make the assumption [5] that in the case of slow burning thick powders at low pressures, the burning layers, notwithstanding their poor heat conductivity, will become heated under the influence of the surrounding gases and high temperature. Due to this increase of temperature at the outer powder layer, the burning reaction, similarly to any other chemical reaction, proceeds the faster, the lower the loading density and gas pressure; the lower the rate ( $u$ ) of displacement of the burning layer towards the center of the grain, the deeper will be the penetration of heat through the layer and the higher will be the temperature of the latter.

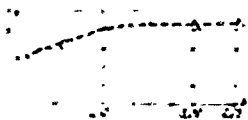


Fig. 83a - The Dependence of  $\int p dt$  on  $\Delta$ .

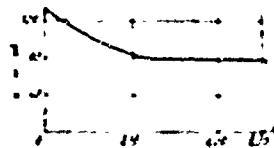


Fig. 83b - The Dependence of  $u_1$  on  $\Delta$ .

1)  $u$  m/sec.

This explanation is qualitatively confirmed by the modern "heat" theory of powder burning developed by Prof. Ya.B. Zeldovich.

A mathematical approach to this phenomenon will show that the divergence of the integral curves  $I, \psi$  at different values of  $\Delta$  can be formally expressed by the burning rate law  $u = Ap^\nu$ , where  $\nu < 1$ .

GRAPHIC NOT REPRODUCIBLE

# GRAPHIC NOT REPRODUCIBLE

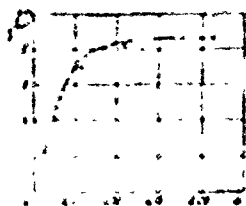


Fig. 84 -  $\int p dt$  as a Function of  $\Delta$ , According to Tests Conducted by Kokhanov.

Our tests with plates with a solid solvent have shown that for  $\Delta > 0.10$  at a pressure of  $p > 1000 \text{ kg/cm}^2$  it may be assumed that for

$$u = u_1 p,$$

$\Delta < 0.10$  and pressure up to  $800\text{--}1000 \text{ kg/cm}^2$  the nature of the variation of  $\int p dt, \psi$  is such that the following law will apply

$$u = A p^\nu,$$

where  $A = 0.240$  and  $\nu = 0.83$ .

Tests conducted by Prof. Yu.A. Pobedonostsev at very low pressures give a relation of the form  $u = ap + b$ :

$$u = 0.063p + 3,$$

where  $u$  is expressed in mm/sec and  $p$  in  $\text{kg/cm}^2$ .

Prof. Ya.M. Shapiro gives the relation  $u = A p^\nu$  for the same test data:

$$u = 0.37 \cdot p^{0.7}.$$

The values of  $u$  are practically the same when computed by means of these formulas for  $p \geq 25-300 \text{ kg/cm}^2$ .

Therefore, for simple shaped pyroxylin powders with a solid solvent, the following burning rate law holds true at  $\Delta > 0.10$  and pressures above  $800 \text{ kg/cm}^2$ :  $u = u_1 p$ .

For these same powders at pressures  $< 800 \text{ kg/cm}^2$ , the appropriate burning rate law is  $u = Ap^\nu$ , where  $\nu < 1$ .

When the pressure  $p$  varies from 300 to  $800 \text{ kg/cm}^2$ , the value of  $\nu$  itself apparently changes also and approaches unity.

Thus the burning rate law is not the same for different conditions of burning; its form changes with change of pressure.

#### B. Applying the Diagrams to Powders with Narrow Perforations

In the case of progressive pyroxylin powders with many narrow perforations the integral curves  $I, \psi$  proceed in the form of a diverging cluster because of the nonuniform conditions of burning in the narrow perforations and at the outside surface, the disposition of the curves being the higher the greater the value of  $\Delta$ . Starting with  $\psi \approx 0.60-0.65$ , the  $I, \psi$  curves become practically parallel (figs. 85 and 86).

# GRAPHIC NOT REPRODUCIBLE

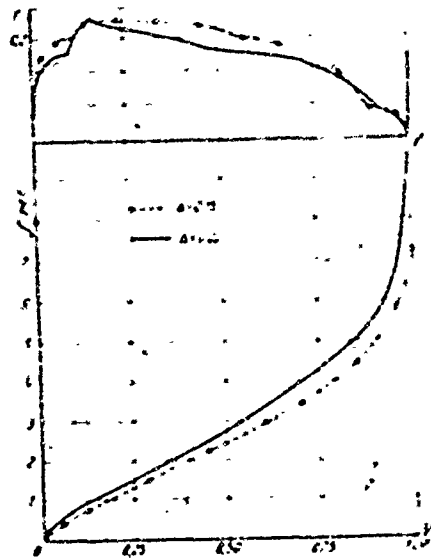


Fig. 85 -  $\int p dt$ ,  $\Psi$  and  $\Gamma$ ,  $\Psi$  Curves for 7/7 Powder.

On the basis of the above criterion for the burning rate law, the divergence of the integral curves cluster leads to the following law:

$$u = Ap^{\nu},$$

where  $\nu < 1$ .

Tests involving a large number of powder specimens (over 100 specimens) consisting of powders with 7 perforations and Walsh's grades 7/7, 9/7, 12/7 and 15/7 give the value of  $\nu = 0.83 \approx 5/6$  for our domestic pyroxylin powders with 7 perforations.

Once again we arrive at an apparent contradiction: for pyroxylin powders of plain shapes (plate and short tube), the burning rate law at  $\Delta > 0.12$  is expressed by the formula

$$u = u_1 p.$$

For the same pyroxylin powders with narrow perforations at the same values of  $\Delta > 0.12$  the burning rate law is expressed by the formula

$$u = Ap^\psi,$$

because the integral  $I, \psi$  curves proceed in the form of a diverging cluster and are disposed on the diagram the higher, the higher is the loading density.

## GRAPHIC NOT REPRODUCIBLE

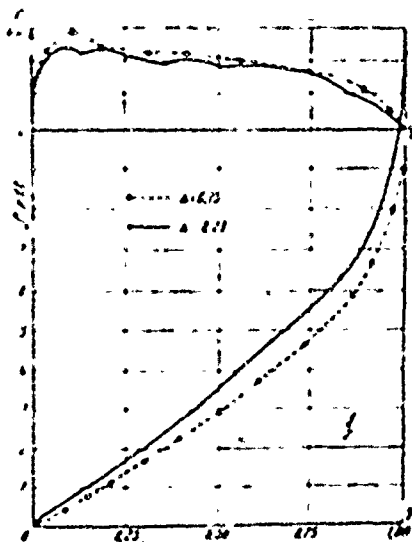


Fig. 86 -  $\int p dt, \psi$  and  $\Gamma, \psi$  Curves for 9/7 Powder.

This apparent contradiction can be easily explained on the



basis of the theory of nonuniform burning. It was shown above that location of the  $\Gamma, \psi$  curves is the lower, the higher the loading density, but  $\Gamma$  is the cotangent of the angle made by the  $I, \psi$  curves with the  $\psi$  - axis; hence, as  $\Gamma$  decreases with the increase of  $\Delta$ , the slope angle of the integral curves increases and they continue to ascend higher and higher in the form of a diverging cluster.

Thus, in the case of the burning rate law  $u = u_1 p$  corresponding to the nature of the powder and the conditions of loading ( $\Delta > 0.12$ ), the integral curves nevertheless proceed as a diverging cluster because of the nonuniform burning of perforated powders at different values of  $\Delta$ . Again, formally this divergence of the integral  $I, \psi$  curves with change of  $\Delta$  can be expressed by the burning rate law

$$u = Ap^{\nu},$$

where  $\nu < 1$ .

The burning rate law for colloidal powders is expressed by the formula

$$u = u_1 p.$$

For powders with a solid solvent  $u_1$  is a constant; for ordinary pyroxylin powders and also for nitroglycerin ones  $u_1$  is a variable in the first third of the burning process; it depends on the nature of the powder and the conditions of burning.

Notwithstanding the fact that  $u_1$  is a variable, the integral  $\int_0^t p dt$ ,  $\psi$  curves have the form of a converging cluster at different values of  $\Delta$ .

Deviation from this law in the form of diverging  $\int p dt, \psi$  curves for powders of simple shapes at small values of  $\Delta$  is explained by the change of the burning rate  $u_1$  due to the heating of powder layers when burning is gradual.

An analogous divergence of the integral curves for progressive powders at large values of  $\Delta$  and the apparent deviation from the  $u = u_1 p$  law is due to the nonuniform pressure distribution in the perforations and at the outside surface of the powder which depends on  $\Delta$ .

This apparent deviation from the  $u = u_1 p$  law can be expressed in a purely formal manner by means of formula  $u = A_1 p^\gamma$ , but the law governing the displacement of the burning surface towards the center of the grain for each element of the powder surface remains the same:  $u = u_1 p$ , where  $p$  may be different at various elements of the surface, and  $u_1$  may vary from layer to layer and will depend on the temperature of the layer near the burning surface. For powders with 7 perforations  $\gamma \approx 0.80-0.83$ , and the  $A$  coefficient depends on the nature of the powder (contains nitrogen and volatiles).

#### Conclusions

The pyrostatic relations and the method of determining the various characteristics, as outlined above, make it possible to obtain a full analysis of the ballistic characteristics of powder and of the true law of combustion from tests in a manometric bomb.

The ballistic characteristics - energy  $f$  and covolume  $\alpha$  - are determined from bomb tests at two or three loading densities by performing 3 to 5 tests at each value of  $\Delta$ .

A correction for heat transfer is introduced into the test data ( $p_{m1}$ ,  $p_{m2}$ ,  $f$ ,  $\alpha$ ) and the corrected values of  $f_0$  and  $\alpha_0$  are determined.

The burning rate,  $u_1$ , at a pressure  $p = 1$  is determined from the analysis of the integral curve  $\int_0^t p dt, \Psi$ :

$$u_1 = \frac{c_1 c_p}{I_1}.$$

The true powder burning law is characterized by the test curve of the intensity of gas formation  $\Gamma = \frac{1}{p} \frac{d\Psi}{dt}$  as a function of  $\Psi$  and  $t$  and by the curve of pressure impulse variation  $\int_0^t p dt$  as a function of the burned portion of the charge  $\Psi$ .

The burning rate law is determined from the convergence or divergence of the cluster of the integral  $I, \Psi$  curves.

The  $\Gamma, \Psi$  curve acts as the analyzer of the processes occurring during burning of powder and permits the evaluation of the various factors involved which could not be disclosed by any other methods (the process of gradual ignition, changes in the burning rate, effects of flegmatization, etc.).

In order to evaluate the burning of powder in the bore of a barrel when the gun is fired, tests must be conducted in a bomb at different but constant loading densities, and a determination made of the effect of loading density on the change in the progressivity of burning. A conclusion can be reached regarding the burning of powder in the gun's bore at a variable volume from the comparison and the analysis of the obtained data.

This entire method of investigation can be called the method of ballistic analysis of powders.

Inasmuch as this method permits determining the changes in the powder composition and in its dimensions under test conditions, it may be found very useful at powder manufacturing plants, particularly in the development of test specimens; when performing bomb tests and comparing the results with regular standard powder specimens it would permit establishing the deviation of the test specimen from standard samples and predicting its actual behavior in firing.

The following formula will serve as an example of the direct application to firing practice of the results of ballistic analysis obtained under laboratory conditions. It permits determining the relative weight of a test specimen from comparative bomb tests of two powder specimens -- a standard and test specimen.

Designating the characteristics:

of the standard specimen -  $\omega'$ ,  $f'$ ,  $I_K'$ ; and

of the test specimen -  $\omega''$ ,  $f''$ ,  $I_K''$ ;

$$\frac{\omega''}{\omega'} = \frac{\frac{f'}{f''} \frac{I_K'}{I_K''}}{1 + \frac{\Delta'}{\delta} \left( \frac{f'}{f''} \frac{I_K''}{I_K'} - 1 \right)},$$

where  $\Delta'$  is the loading density of the standard specimen in a gun.

In order to avoid the errors usually obtained in taking the complete integral  $I_K$  until the end of burning, it is preferable to take the values of  $\int_{0.05}^{0.75} p dt$  for  $I'$  and  $I''$ ; by disregarding the

initial section up to  $\psi = 0.05$ , the variation in ignition obtained with the use of relatively weak igniters ( $p_g < 50 \text{ kg/cm}^2$ ) will be eliminated.

The above formula permits determining without firing the approximate weight of a test powder specimen developing the same maximum gas pressure and muzzle velocity as a standard specimen.